Dielectric Modeling of Hydrated Cement Paste Panels

BY

Hao Liu
Bachelor of Engineering, Chongqing University (2007)

SUBMITTED IN PARTIAL FULFILLMENT OF THE REQUIREMENTS
FOR THE DEGREE OF MASTER OF SCIENCE
DEPARTMENT OF CIVIL AND ENVIRONMENTAL ENGINEERING
UNIVERSITY OF MASSACHUSETTS LOWELL

Signature of the Author .....
Department of Civil and Environmental Engineering
May, 2013

Signature of Thesis Supervisor .....
Dr. Tzu-Yang Yu
Assistant Professor

Committee Member Signature .....
Professor Donald Leitch
Department of Civil and Environmental Engineering

Committee Member Signature .....
Professor Susan Faraji
Department of Civil and Environmental Engineering

Dielectric Modeling of Hydrated Cement Paste Panels

BY

Hao Liu
Bachelor of Engineering, Chongqing University (2007)

ABSTRACT OF A THESIS SUBMITTED TO THE FACULTY OF THE
DEPARTMENT OF CIVIL AND ENVIRONMENTAL ENGINEERING
IN PARTIAL FULFILLMENT OF THE REQUIREMENTS
FOR THE DEGREE OF
MASTER OF SCIENCE
UNIVERSITY OF MASSACHUSETTS LOWELL
2013

Thesis Supervisor: Dr. Tzu-Yang Yu
Title: Assistant Professor

Dielectric properties of cementitious materials (cement paste, cement mortar, and concrete) are key parameters in radar simulation and radar sensor are used in condition assessment of structures in Civil Engineering as one non-destructive testing (NDT) method. However, due to heterogeneity of cementitious materials, it is difficult to understand, measure and model dielectric properties of these materials. In this thesis, several dielectric models were applied on oven-dried and room-condtioned hydrated cement paste panels. Modeling results are used for fitting experimental results obtained using open-ended coaxial probe at room temperature 21-25°C with 25-30% relative humidity. In use of homogeneous models, dielectric constant of cement paste panels at the frequency of zero and infinity, and relaxation time were calculated and compared. In use of heterogeneous models, how shapes of inclusion materials and selection of host and inclusion material influence dielectric properties of mixing material was also investigated.

Acknowledgements

First, sincere and forever thanks will go to my family for their unmeasured support.

I also would like to express my deepest thanks to my research advisor, Dr. Tzuyang Yu, who has enhanced my ability with his enormous and endless hard work.

As well, I want to thank my thesis committee members, Professor Leitch and Professor Faraji for their invaluable comments.

In addition, I appreciate financial support from VOTERS (Versatile Onboard Traffic-Embedded Roaming Sensors) sponsored by National Institute of Standard and Technology (NIST) Technology Innovation Program (TIP) during my study.

Finally, I have my best wishes to my partners who were always helping me, Carlos Jaquez, Justin Wilson, Ross Gladstone, Shafique Ahmed and CheFu Su.

Contents

List of Figures

List of Tables

Chapter 1

Introduction

The health and integrity of civil infrastructure are important to ensure public safety. However, deterioration of structures is an inevitable process in their lifespan. In order to determine health condition and to predict service life of structures without any new damages to structures, non-destructive testing (NDT) methods (e.g., radar, acoustic sensors, ultrasonic sensors, electrochemical sensors) have become a popular research topic because of their advantages over traditional testing methods. Among these methods, radar is one electromagnetic method which can be used for the assessment of structural health by collecting reflected electromagnetic (EM) wave from a medium, such as cementitious materials which are dielectrics, since the properties of EM waves change within different medias. Analysis of subsurface condition can be achieved by comparing parameters (e.g. travelling time, phase velocity and signal attenuation). Nevertheless, some parameters of material properties which are important to radar simulation, for example dielectric properties of cementitious materials, are measured in in-direct methods or simply assumed, which may result in misleading of structure assessment.

Dielectric properties of cementitious materials are critical to radar simulation because they are used for estimation of phase velocity of EM wave and energy attenuation during propagation of EM wave within structures [4, 6, 7, 13, 14]. Therefore, accurate measurements on dielectric properties of cementitious materials are required. In the recent research work done by Solak (2011) [25], how to measure dielectric properties of hydrated cement paste panels and cement mortar panels using an open-ended coaxial probe and the reliability of measurements were investigated. Better understanding and application of dielectric modeling on cementitious materials will improve accuracy of radar test and verify experimental results.

Dielectric properties of hydrated cementitious materials are determined by the components and the proportions. The effects of the water-to-cement (w/c) ratio, air void ratio and types of fine and coarse aggregates on dielectric properties are not clearly understood. Due to high number of uncertain factors, it is challenging to model or measure dielectric properties of cementitious material.

Hydrated cement paste has solid phase which is only hydrated cement paste, gaseous phase, and possibly liquid phase. It is considered as the simplest cementitious material. Dielectric models are used to verify experimental results and to calculate other parameters for radar simulation (e.g., dielectric constant at frequency of zero and infinity, relaxation time). Also, research work of dielectric modeling on hydrated cement paste panels will provide a basis and direction for modeling on more complicated cementi-

tious materials, such as cement mortar and concrete.

1.1 Research Objective

The objective of this research is to develop dielectric models for hydrated cement paste panels to predict the dielectric properties of hydrated cement paste, considering different w/c ratios, moisture contents and measurement frequencies. Such knowledge can help to better understand the inspection data using electromagnetic sensing devices such as radar.

1.2 Thesis Approach

In this thesis, dielectric models for both homogeneous and heterogeneous material are used for modeling dielectric properties of hydrated cement paste panels. The input data is from experimental measurements using an open-ended coaxial probe collected by Solak (2011) at room temperature 23-25°C with 25-30% relative humidity [25]. The road map of this thesis is shown in Figure 1-1.

Debye's model, Havriliak-Negami's model and Yu's model are dielectric models for homogeneous materials from the theory of dielectric dispersion. We know that dielectric properties of cementitious materials depend on combination of dielectric constants at the frequencies of zero and infinity, relaxation time, as well as the w/c ratio. In Debye's model, the curves of relaxation time with frequency is obtained by assuming

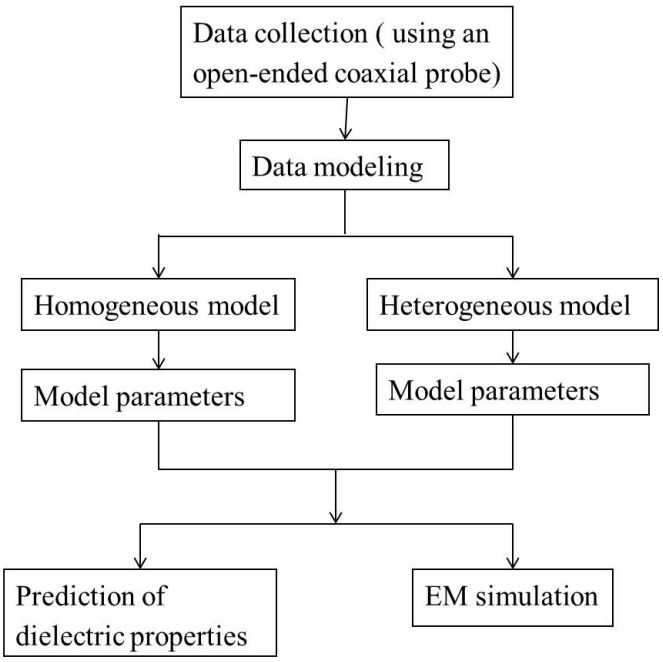

Figure 1-1: The road map of the theis

dielectric constant at infinite frequency. When the initial curve which decreases with frequency at the beginning but increases in the end shows up, the assumed dielectric constant at the frequency of infinity is identified as the real value. Then dielectric constant at the frequency of zero and relaxation time were obtained in the case that there is lowest norm error between experimental results and modeling results. In addition, how dielectric constant at the frequency of zero and infinity as well as relaxation time are influenced by w/c ratio is examined. Havriliak-Negami's model is one robust version of Debye's model with an extra parameter which can make modeling results closer to experimental results. The procedure is similar as that of Debye's model. In Yu's model, w/c ratio is involved since it is an important parameter for cementitious materials which can influence hydration products and air-void ratio.

Maxwell-Garnett's model, Weiner's model, and Polder-van Santen's model are for heterogeneous materials. Maxwell-Garnett's model is used in its inverse way, and it is used for examining how selection of host material and inclusion material influences overall dielectric properties. At the same time, its effectiveness on hydrated cement were verified by statistical methodology. Weiner's model is a two-phase model, which is for the inclusion material with arbitrary shapes. Different shapes of the inclusion material have different dispersion factors. How shapes of the inclusion material influence overall dielectric properties is examined by assuming different shapes and their dispersion factors. Polder-van Santen's model is a multi-phase model and it is used for modeling dielectric properties of room-conditioned cement paste panels. It is assumed that the shape of air is either needle or sphere. Also the depolarization factors of water need to be assumed.

1.3 Organization of the Thesis

The organization of this thesis is as follows.

Chapter 2 reviews the applications of dielectric properties in civil engineering, and measurement of dielectric properties on cementitious materials, as well as dielectric models.

Chapter 3 introduces the design of cement paste panels and the experimental work to collect dielectric data from hydrated cement paste panels.

Chapter 4 describes the use of homogeneous models on hydrated cement paste panels and the performance of the models.

Chapter 5 describes the use of heterogeneous models on hydrated cement paste panels and the performance of the models.

Chapter 6 summarizes the research findings and recommends future work.

Chapter 2

Literature Review

The use of dielectric properties in civil engineering as well as dielectric measurements on cementitious materials have been studied by many researchers. However, practical modeling results on cementitious materials are limited.

Dielectric properties can be used for identifying structural characteristics in civil engineering. For example, by using ground penetrating radar (GPR), characteristics of reinforced concrete (RC) structures (e.g., radius of rebar, moisture content), can be estimated from dielectric properties or the difference of materials [6, 8]. In addition, water content in fresh and hardened concrete can be estimated by dielectric measurements.

Dielectric measurements on cementitious materials are also studied by researchers using different test methods on samples of different shapes and sizes, as well as in different frequency ranges. Reported methods include coaxial transmission line, waveguide, resonator cavity, and free space [25]. The main objective of dielectric measurements in this thesis is to i) experimentally determine dielectric properties of cementitious materials and ii) to find out how dielectric properties of cementitious materials are influenced

by such as w/c ratio, moisture content, and air void ratio in the material.

Meanwhile, in order to perform numerical simulation of the radar response of RC structures, dielectric models of cementitious materials are needed. In fact, some dielectric models were developed long time ago, but they were not originally developed for cementitious materials. In these models, complexities of cmentitious materials were not considered. Due to the complexities and lack of experimental data, effectiveness of these models on cementitious materials has not been verified, even though there were some positive results. In this thesis, several existing dielectric models are verified by fitting dielectric properties of cement paste panels which is the simplest cementitious material. The input data of dielectric models is the experimental results collected by Solak using open-ended coaxial probe connected with HP 5071C network analyzer.

Therefore, in this chapter, applications of dielectric properties in civil engineering, dielectric measurement on cementitious materials as well as dielectric models are reviewed.

2.1 Applications of Dielectric Property in Civil Engineering

Dielectric properties determine the propagation of EM waves inside materials, such as the phase velocity of EM wave, and amplitude of EM waves [6]. Also, dielectric properties were used for estimating the moisture content and the depth of material[8]. These characteristics can help identifying structural properties.

Janoo *et. al.* (1999) [11] developed an equation to correlate the dielectric constant of concrete and volumetric water content for concrete. This equation was effective for volumetric water content in the range of 4% to 11%, which covers a wide range of volumetric water content in the field. In their opinion, more curves between dielectric constant and volumetric water content have to be developed to estimate the volumetric water content in concrete.

Laurens *et. al.* (2002) [14] examined how relative humidity within concrete influences radar signal. Radar images show that the amplitude of the first peak increases with the loss of moisture within 69 days drying after mixing. Also, we know that loss of moisture content leads to lower dielectric constant reported by Soutsos *et. al.* (2001) [26] and Solak. Therefore, dielectric constant affects the amplitude of first peak of radar signal.

Al-Qadi *et. al.* (2001) [4] evaluated how dielectric properties of different layers of hot-mix asphalt and concrete influence radar signal. The test was performed on Virginia Smart Road with different layers of materials. From the measured radar signal, it was concluded that lower dielectric contrast between different layers will lead to relatively low reflection.

Chang *et. al.* (2009) [7] measured the radius of reinforced steel bars in concrete from dielectric contrast of different materials in RC structures using GPR images. From the reflected signal, higher amplitudes were generated the interface between steel rebar and concrete. This was also consistent with results by Al-Qadi *et. al.* (2001) [4].

Lai *et. al.* (2009) [13] characterized dielectric properties of concrete with drying process using GPR. The results show that GPR amplitude of the first wave increases

with the loss of moisture which is the same as the conclusion from Laurens *et. al.* (2002) [14]. In addition, it is reported that higher water to binder ratio can lead to higher dielectric constant within 100 days after mixing as well.

Chen *et. al.* (2012) [8] developed an equation to correlate the water content in fresh concrete with the dielectric constant of concrete measured by GPR. In their work, the equation was derived from a hybrid capacitor model by assuming concrete to be a 3-phase material (solid phase, water phase and air). Dielectric constant of concrete was calculated from the phase velocity of EM wave within concrete. The phase velocity of EM wave in concrete was identified using a GPR system connected with 1.5 GHz antenna by propagation time of EM impulse.

2.2 Dielectric Measurements on Cementitious Materials

De Loor (1961) [15] investigated the effect of moisture on the dielectric constant of hardened cement paste. Disc-shaped cement paste samples were cast with w/c ratios of 0.26, 0.31, and 0.36. Dielectric constant was measured in the frequency range of 0.1 MHz to 10 MHz, using a condenser consisting of two electrodes. Also, dielectric constant data was collected at the frequencies of 3000, 3750, 7450 and 9375 MHz with a coaxial waveguide system. From his experimental results, dielectric constant of hardened cement paste increases with the increase of moisture content. Additionally, the dielectric constants of cement paste is higher at lower frequency if the same method

was used and the age of cement paste was the same.

Al-Qadi *et. al.* (1995) [3] measured the dielectric properties of portland cement concrete using an HP 4195A network analyzer connected with a parallel plate capacitor. Dielectric properties were measured in moisture curing time in the frequency range of 0.1MHz to 40MHz. It was found that the dielectric constant of concrete decreases with the curing time. Also, the dielectric constants decreased with the increase of frequency.

Robert (1998) [21] obtained dielectric data of concrete using a coaxial line from 50 MHz to 1 GHz. He also examined the influence of sodium chloride on the dielectric properties of concrete. It was observed that dielectric constants of concrete showed a descending trend with the increase of frequency. It was also found that, chloride had a significant effect on the dielectric properties of concrete when the frequency was lower than 1 GHz. But if the frequency was higher than 1 GHz, the influence from chloride disappeared.

Janoo *et. al.* (1999) [11] reported the dielectric properties of cement mortar contributed from different components (moisture, air, cement paste, and sand). Cement mortar samples were cast in cylindrical model with the diameter of 76 mm and the height of 152 mm. The w/c ratio of cement mortar samples was 0.41. Dielectric constant was measured using Time Domain Reflectrometry (TDR) probes which were embedded in fresh cement mortar samples. It is found that, moisture has a significant effect on the overall/effective dielectric constant of cement mortar because it has the higher dielectric constant among than other materials in cement mortar.

Wen *et. al.* (2001) [28] evaluated how admixtures influence the dielectric constant of cement paste. Testing method in their paper was the parallel-plate capacitor method

in the frequency range of 10 kHz to 1 MHz. Several types of cement paste samples with different admixtures (e.g., silica fume, latex, steel fibers, and carbon fibers) in different proportions were prepared. The w/c ratios of the cement paste samples were 0.23 and 0.35. Comparing dielectric constants of cement paste with the same admixture at different frequencies, it was found that the dielectric constants at higher frequency were lower. Experimental results showed that the dielectric constant of cement paste increased with the addition of latex and carbon fibers. Nevertheless the dielectric constant of cement paste decreased with the addition of silica fume and steel fibers.

Soutsos *et. al.* (2001) [26] used an HP 8753B network analyzer connected with a transmission line to measure the dielectric properties of concrete with the change of volumetric water content in the frequency range of 10 MHz to 1000 MHz. It was observed that the dielectric constant of concrete decreased with the decrease of moisture content in concrete matrix and moisture content seems to be the dominant factor to influence dielectric properties of concrete. Also, the dielectric constant of concrete decreased with the increase of frequency.

Wen *et. al.* (2002) [29] measured the dielectric constant of cement paste samples using the two-probe method and an RLC meter (QuadTech 7600) in the frequency range of 10 kHz to 1 MHz. The samples were cast in the form of cylindrical disks with a 12.3 mm diameter and a 2 mm thickness, and the w/c ratio was 0.35. The sample was demolded 24 hours after casting and cured in room condition with relative humidity of 100% for 28 days. Dielectric constant was measured with compressive force applied on the cement paste samples. It was observed that the dielectric constant of cement paste increased nonlinearly with the compressive stress (up to 6.4 MPa) inside the paste. But

the dielectric properties of cement paste did not return to the original value when the compressive loading was released.

Sagnard *et. al.* (2005) [22] performed dielectric measurements on oven-dried cement mortar using the free-space method in an anechoic chamber in the frequency of 8 GHz to 12.5 GHz. The sample dimensions were 17 cm by 17 cm with a thickness of 4 cm. It was observed that the dielectric constant of oven-dried cement mortar decreased with the increase of w/c ratio. This was because higher w/c ratios lead to higher porosities while air has the lowest dielectric constant.

Makul *et. al.* (2010) [16] investigated the dielectric properties of cement paste, cement mortar and concrete during the first 24 hours after casting by using a network analyzer connected with an open-ended coaxial probe at the frequency of 2.45 GHz. The w/c ratios of concrete in this paper were 0.38, 0.45 and 0.70, while the w/c ratio of cement paste and cement mortar was 0.38. It was observed that the dielectric constant of cement-based material changed little during the dormant period since the chemical compositions of the aqueous remained constant, and that the dielectric constant was relatively high. However, dielectric constant decreased quickly after dormant period when hydration reaction resumes. In addition, from the results of dielectric constant on concrete with different w/c ratios, it was found that the dielectric constant decreases with the decrease of w/c ratio during 24 hours after casting. Also, through the comparison on dielectric constant of cement paste, cement mortar and concrete, it was found that plain cement paste had the highest dielectric constant while concrete had the lowest if the w/c ratio was the same due to the lower dielectric constant of aggregate.

2.3 Dielectric Modeling

Bungey (2004) [6] reviewed dielectric models and measurements on concrete. Dielectric properties do have significant influence on phase velocity of EM waves within concrete. In addition, experimental work in lab environment confirmed several factors and their influences on dielectric properties. However, as to dielectric modeling, limited practical outcome has reported due to complexity involved in concrete.

Sihvola *et. al.* (1988) [24] proposed a dielectric model for heterogeneous materials and examined how inclusion materials with different shapes scatter in host material influence the overall dielectric properties of snow and sea ice. From their paper, shapes of inclusion materials influenced the overall dielectric properties by changing dispersion factor which is an important parameter in dielectric modeling of heterogeneous materials. Their model was applied on snow and sea ice by assuming the shapes of inclusion materials to be elliptical. The results from the model were in good agreement with Maxwell-Garnett's model.

Tsui *et. al.* (1997) [27] presented several heterogeneous models and compared these models by assuming the loss factor of concrete to be zero. In their paper, heterogeneous models are classified into two categories: volumetric models and geometric models. Volumetric models considered volume fractions of constituents, but geometrical models considered not only volume fractions but also shapes of inclusion materials. The effectiveness of the models were not verified since there was no experimental data.

Robert (1998) [21] obtained dielectric data of concrete using a coaxial line from 50 MHz to 1 GHz and applied five dielectric models for data fitting; including Cole-

Cole's model, Debye's model, double layer polarization, CRIM (complex refraction index model), and self similar model. Among these five models, Cole-Cole's model provided the best performance on fitting experimental data.

Mantas (1999) [17] extended Debye's model for the relaxation behavior of dielectrics by including two or three types of dipoles, and each type has its relaxation time. The material used in his paper was ceramics. Fractions of the dipole types to overall polarization were needed in his model. It was concluded that if relaxation times for different dipoles are used, rather than distribution relaxation times, better results can be obtained.

Hager III *et. al.* (2004) [10] took dielectric measurements on cement paste from initial mixing to several weeks of curing in the frequency range of 10 kHz to 8 GHz. In their paper, Debye's model was used for fitting experimental results. Modeling results showed similarities with Miura *et. al.* (1998) [18] who performed dielectric measurements on cement paste using TDR method at around 100 MHz. Also there were similarities between modeling results and experimental results by Hafiane *et. al.* (1999) [9] in the frequency range of 1 MHz to 1.8 GHz.

Ogunsola *et. al.* (2006) [19] used an extended Debye's model to fit experimental results done by Soutsos *et. al.* (2001) [26] and Robert (1998) [21]. In the extended Debye's model, direct current (DC) conductivity of concrete was considered. Dielectric constants at the frequencies of infinity and zero, relaxation time and DC conductivity were obtained from curve fitting. It was found that moisture content was a very important factor to model parameters. Dielectric constants at the frequencies of infinity and zero and DC conductivity all increased with the increase of moisture content in the

range of 0 to 12%.

Sandrolini *et. al.* (2007) [23] applied an extended Debye's model on concrete with different moisture contents in the frequency range from 0.1 GHz to 2 GHz. Experimental results were obtained by using a coaxial transmission line. Debye's parameters were calculated from curve fitting on experimental results. It was also found that the dielectric constant at the frequencies of infinity and zero and direct current (DC) conductivity all increase with the increase of moisture content. Additionally, the authors pointed out that DC conductivity should be considered in the imaginary part of dielectric properties.

Klysz *et. al.* (2008) [12] evaluated dielectric constant of concrete by a Finite-Difference-Time-Domain (FDTD) model. Experimental data was obtained from nine concrete samples by using GPR at the frequency of 1.5 GHz. The dielectric constants from experimental data and FDTD modeling were very close. In addition, how dielectric constant and DC conductivity influence the travelling time and amplitude values of GPR signals were examined.

2.4 Summary

In this chapter, application of dielectric properties in civil engineering, dielectric measurements on cementitious materials as well as dielectric models are reviewed. From review, we can find that dielectric properties of cementitious materials can be used for identifying structural characteristics. In addition, dielectric properties are influenced by many factors from material itself, such as moisture content and w/c ratio, as well as frequency of equipment. It is found that dielectric properties of cementitious materials

increase with the increase of moisture content and higher w/c ratio could lead to higher dielectric constant at the same frequency. On the other hand, dielectric constant shows a descending trend with the increase of frequency. However, there are not many papers about dielectric modeling on cementitious materials. The validity of current models (e.g., Debye's model, Cole-Cole's model, Maxwell-Garnett's model) will have to be examined in order to be applied on cementitious materials. Because the models were not originally developed for cementitious materials and the complexities of cementitious materials were not considered.

Chapter 3

Experimental Measurements

The input data for dielectric modeling is from the experimental measurements on hydrated cement paste panels using an open-ended coaxial probe, which was collected by Solak [25]. In this chapter, dielectric measurements on hydrated cement paste panels are explained. In addition, how to design cement paste panels based on research objective and the requirements for measurements is also reported.

The dielectric data was collected from hydrated cement paste panels with different w/c ratios of 0.35, 0.40, 0.42, 0.45, 0.5, and 0.55 in the frequency range of 0.5 GHz to 4.5 GHz with the interval of 0.04 GHz. The size of cement paste panels was 1-foot-by-1-foot-by-1-inch. An Agilent® E5071C ENA series network analyzer, along with an Agilent® 85070E open-ended coaxial probe, was used for collecting dielectric data.

3.1 Sample Preparation

Considering the factors influencing dielectric properties and experimental setup, cement paste panels were prepared based on several considerations in the following.

First of all, from the literature review in Chapter 2, w/c ratio is one important parameter which can influence the dielectric properties of hydrated cement paste panels. To evaluate the how w/c ratio influences dielectric properties of cement paste and model parameters, samples with w/c ratios of 0.35, 0.40, 0.42, 0.45, 0.5, and 0.55 were cast. The specimens used in this thesis are shown in Table 3.1. On the other hand, to eliminate uncertain factors from material, Quikrete® Type I Portland Cement was used for casting all cement paste panels.

Table 3.1: Cement Paste Sample Set

Cement Paste	
W/C	Sample
0.35	CP35
0.40	CP40
0.42	CP42
0.45	CP45
0.50	CP50
0.55	CP55

Secondly, the dielectric properties are very sensitive to moisture content in hydrated cement paste panels. Therefore, dielectric measurements were performed on each cement paste panel twice, before and after oven drying. To avoid cracking on the surface during the process of oven drying, it took two hours to increase from room temperature to 105°C, and it took one hour to decrease from 105°C to room temperature. The whole process of oven drying will take around 24 hours. The detailed steps for oven-drying

are shown in Figure 3-1.

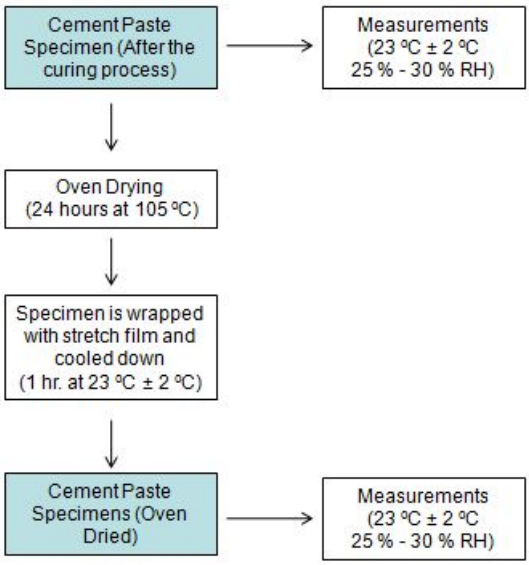

Figure 3-1: Process of oven drying (Source: Solak)

Thirdly, for solid cement paste panels, the accuracy of dielectric properties obtained by open-ended coaxial probe highly depends on the connection between solid phase and probe face. Air gap between solid phase and probe face due to non-perfect connection will increase the ratio of air in measurement medium and decrease the results significantly. Therefore the surfaces of cement paste panels have to be at least as flat as the probe face [1]. In order to have very smooth surface when cement paste panels become hardened, the inner surfaces of the mold were designed to be covered with plexiglass. The dimensions of inner mold is 1 foot in length by 1 inch in width by 1 foot in depth. Figure 3-2 shows the mold and plexiglass in the inner surfaces.

The cement paste panels were demolded after keeping them in the mold under room condition for one day. Then the panels were submerged into water and cured for seven days. After that, the panels were removed from water and placed in room conditions for

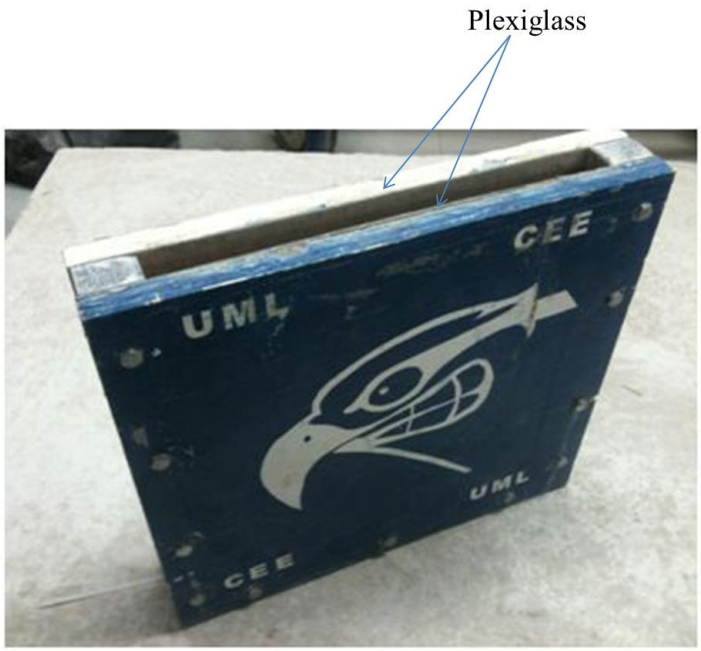

Figure 3-2: The mold with inner plexiglass surface

three months before performing dielectric measurements on them. The room condition here is 21-25°C with 25-30% relative humidity.

3.2 Coaxial Probe Measurement

From literature review of Chapter 2, we know that dielectric properties are frequency dependent. The input data for dielectric modeling is from the measurements using Agilent® E5071C ENA series network analyzer connected with Agilent® 85070E open-ended coaxial probe in the frequency range of 0.5 GHz to 4.5 GHz with the interval of 0.04 GHz. The schematic and the actual picture for experimental setup are shown in Figure 3-3 and Figure 3-4, respectively.

Before taking dielectric measurements on any sample, calibration of the probe has

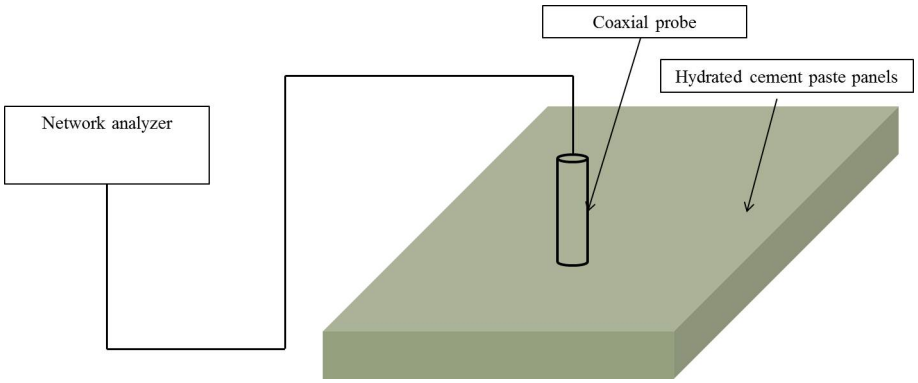

Figure 3-3: Schematic for experimental setup of dielectric measurement on cement paste panels

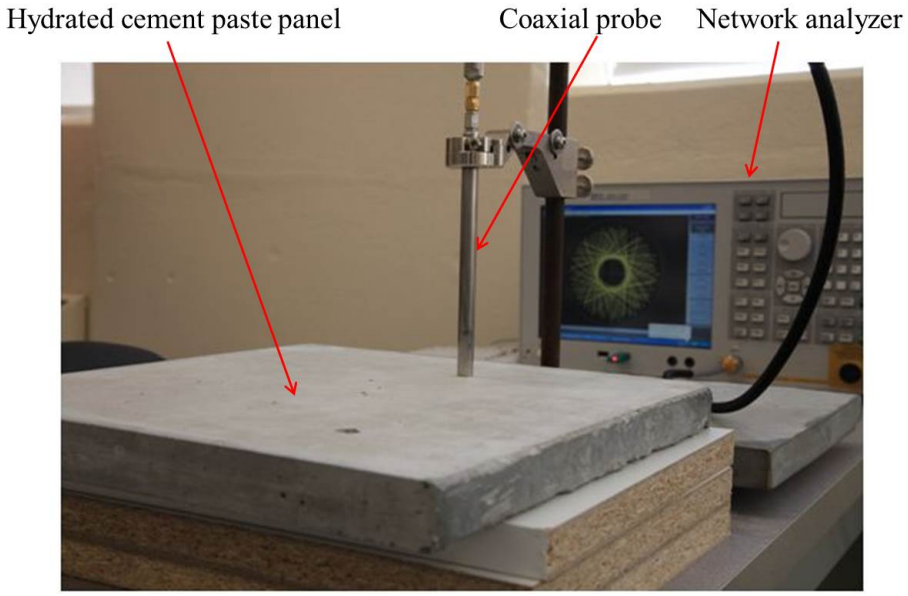

Figure 3-4: Experimental setup of dielectric measurement on cement paste panels

to be performed in order to eliminate the repeatable errors from the measurements. The three known standards, including air, the kit, and water, are used for calibration. The calibration kit and the detailed size of the probe are shown in Figure 3-5 and Figure 3-6.

After calibration, there are still three sources of errors from the dielectric measure-

Figure 3-5: Calibration kit and coaxial probe [2]

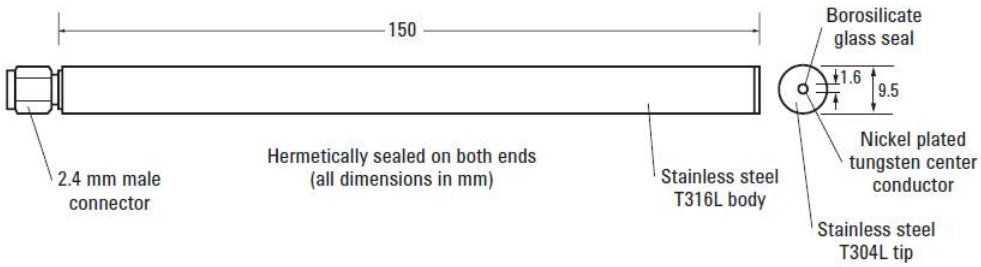

Figure 3-6: Detailed size of the coaxial probe [2]

ments: air gap, cable stability and environmental factors. In order to eliminate the air gap, cement paste panels were cast in the mold with plexiglass in the inner surface. Also, visual inspection on the gap between the surface of the cement panel and the bottom of the coaxial probe was carefully applied every time. On the other hand, to avoid the unexpected influence from environment, the measurements were performed in a relatively stable environment. The room temperature was 23-25°C with 25-30% relative humidity.

Since the diameter of coaxial probe is 0.96 cm such that one dielectric measurement using open-ended coaxial probe was from only one point on the surface of ce-

ment paste panels which may reflect only local condition and neglect the heterogeneity of cementitious material, sixty measurements were taken and average of these sixty measurements was calculated. The reliability of dielectric data was verified by Solak using Yu's method [25]. In this thesis, the input dielectric data is always the average value.

3.3 Summary

In this chapter, how to design cement paste samples based on the objective of research and experimental setup is explained. Also, dielectric measurements on cement paste panels were briefly reported. Reliable dielectric data were obtained as the input data for dielectric modeling.

Chapter 4

Results of Homogeneous Dielectric Models on Cement Paste Panels

In this chapter, homogeneous dielectric models are used for modeling dielectric properties of cement paste panels. The models used in this chapter include Debye's model, Havriliak-Negami's model, and Yu's model. The process and results of modeling are introduced, and the comparison between modeling results and experimental results are made as well.

4.1 Debye's Model

4.1.1 Approach of Debye's Model

In Debye's model, external field approach is used for modeling dielectric properties of cement paste panels. This is because dielectric data was obtained by using open-ended

coaxial probe in macroscopic level and external method can avoid the difficulties on assuming the distribution of internal electrical field. The flowchart to apply Debye's model is show in Figure 4-1.

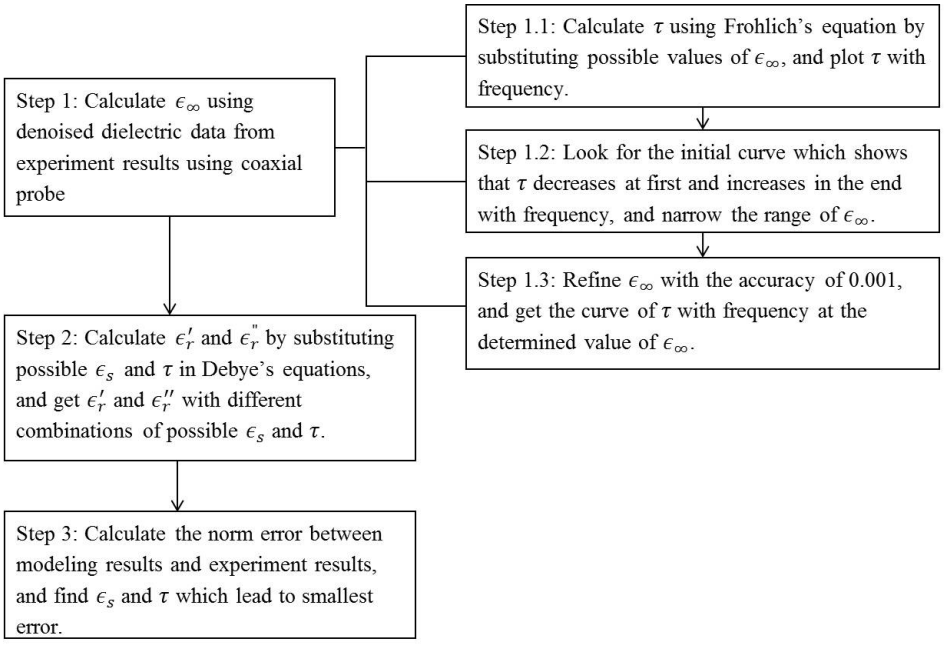

Figure 4-1: Process of Debye's model

From the process of Debye's model, dielectric constant at the frequency of infinity (ϵ_∞) has to be determined first by observing the curves of relaxation time (τ) with frequency. The equation of τ is shown in Eq. 4-1. First, ϵ_∞ is assumed to be a series of values which is less than the smallest value of dielectric constant obtained from experimental measurements in the frequency range of from 0.5 GHz to 4.5 GHz since dielectric constant decreases with the increase of frequency. Then plug assumed ϵ_∞ into Eq. 4-1 and plot τ with frequency by increasing ϵ_∞ at each assume value of ϵ_∞. The curves at a certain assumed ϵ_∞ decrease with the increase of frequency when the assumed value of ϵ_∞ is far away to actual value of ϵ_∞. When the first curve of τ with

frequency which decreases first but increases at the end shows up, the value of ϵ_∞ is determined as the value of ϵ_∞.

$$\tau = \frac{\epsilon_r''}{\omega \times (\epsilon_r' - \epsilon_\infty)} \tag{4.1}$$

where,

τ = Relaxation time (ns)

ϵ_r'' = Loss factor from measurement (Imaginary part of dielectric properties)

ω = Frequency (GHz)

ϵ_r' = Dielectric constant from measurement (Real part of dielectric properties)

ϵ_∞ = Dielectric constant at frequency of infinity

After obtaining the determined value of ϵ_∞, we can get one final curve of τ at different frequencies, from which we can pick up the final value of τ. Assuming possible values of dielectric constant at the frequency of zero (ϵ_s) which is greater than the largest value from experimental measurements, we can get dielectric properties by plugging in different combination of τ and ϵ_s in Eq. 4-2. Finally, τ and ϵ_s are determined by the combination leading to the smallest sum of norm error (NE) from both real and imaginary parts of dielectric properties between experimental results and modeling results. The equation of NE is shown in Eq. 4-3. It should be noted that the best modeling results are defined as the modeling results leading to the smallest NE.

$$\epsilon(\omega) = \epsilon_\infty + \frac{\epsilon_s - \epsilon_\infty}{1 + i \times \omega \times \tau} \tag{4.2}$$

where,

$\epsilon(\omega)$ = Dielectric properties from modeling

ϵ_∞ = Dielectric constant at frequency of infinity

ϵ_s = Dielectric constant at frequency of zero

i = Symbol of imaginary number

ω = Frequency (GHz)

τ = Relaxation time (ns)

$$NE = sum(abs((\epsilon'(\omega) - \epsilon_r'(\omega))) + sum(abs((\epsilon''(\omega) - \epsilon_r''(\omega))) \quad (4.3)$$

where,

NE = Norm error between modeling results and results from experimental measurements

$\epsilon'(\omega)$ = Dielectric constant from modeling at a certain frequency

$\epsilon_r'(\omega)$ = Dielectric constant from measurement at a certain frequency

$\epsilon''(\omega)$ = Loss factor from modeling at a certain frequency

$\epsilon_r''(\omega)$ = Loss factor from measurement at a certain frequency

4.1.2 Results of Debye's Model on Oven-dried Cement Paste Panels

In this section, oven-dried CP35 is used as an example to show the results of Debye's model step by step. The modeling results from oven-dried cement paste panels with the

other w/c ratios are also reported and discussed.

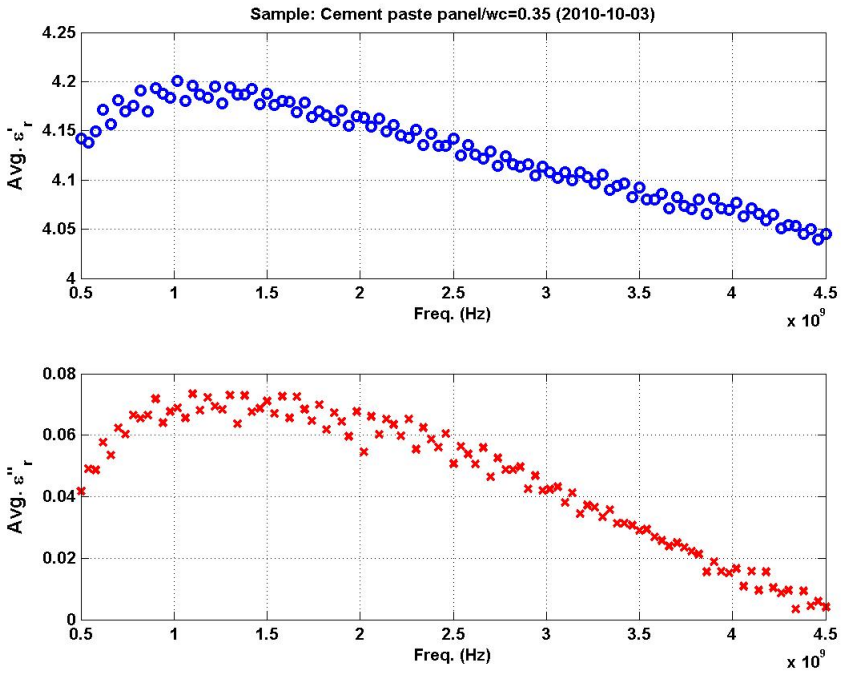

Figure 4-2: Experimental results on oven-dried CP35

Figure 4-2 shows the dielectric constant and loss factor from experimental measurements on oven-dried CP35. The data from 0.5 GHz to 0.98 GHz was removed since it increases with the increase of frequency which is against the theory of dielectric dispersion, and was not considered to be accurate.

According to the steps of Debye's model, ϵ_∞ for CP35 is determined as 4.035 from Figure 4-3. We can see that the curves of τ with frequency started to increase at the end of frequency from ϵ_∞=4.035 which is the determined value of ϵ_∞. The final curve of τ with frequency at ϵ_∞=4.035 was obtained as well.

After determining ϵ_∞ and final curve of τ at different frequencies, dielectric properties from Debye's model were calculated by plugging τ and assumed ϵ_s into Eq. 4-2.

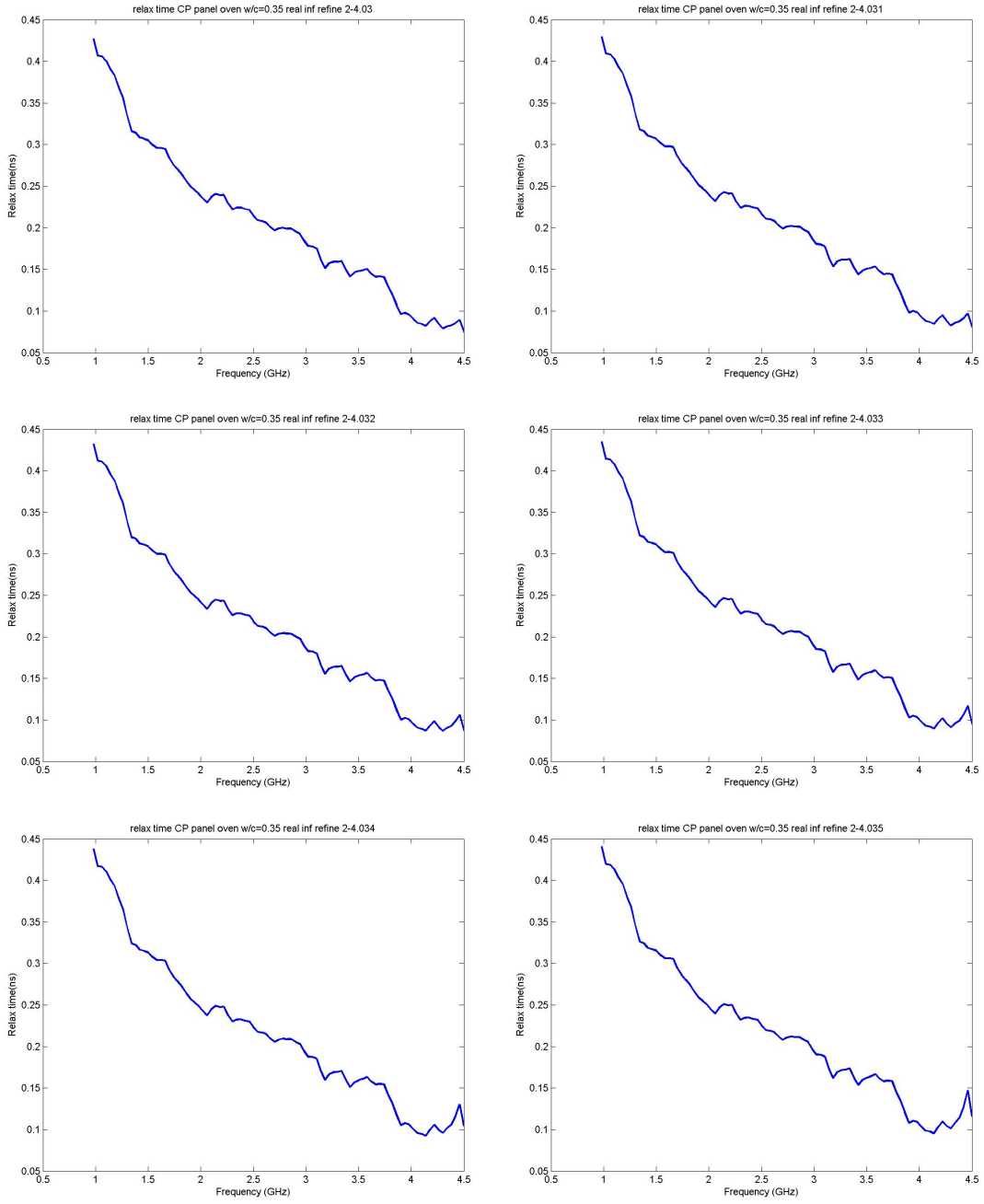

Figure 4-3: Relaxation time with frequency for oven-dried CP35 - ϵ_∞=4.030 to ϵ_∞=4.035

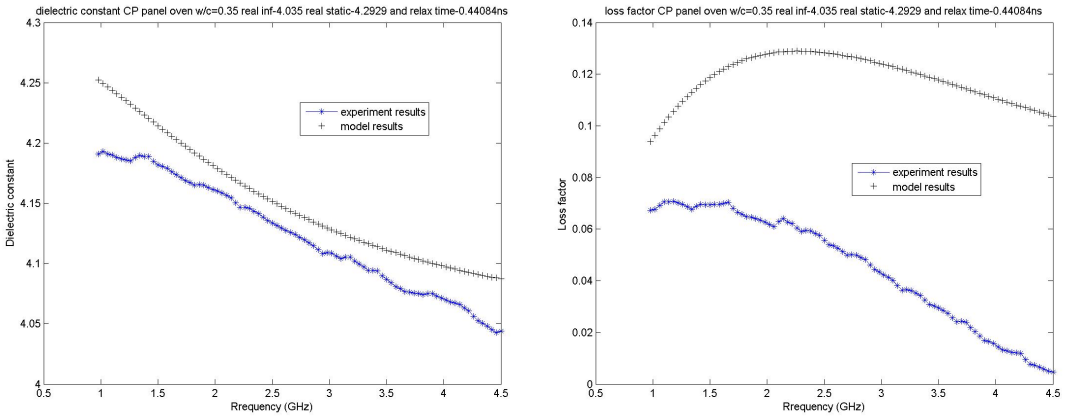

Figure 4-4: Results of dielectric properties for oven-dried CP35 from Debye's model

At the same time, NE was calculated by using Eq. 4-3. The combination of τ and ϵ_s leading to the smallest NE was the determined value of τ and ϵ_s. The determined values of τ and ϵ_s are 0.4408 ns and 4.2929, respectively.

Figure 4-4 shows the best overall performance from Debye's model on dielectric properties of oven-dried CP35. We can see that the modeling results of loss factor on oven-dried CP35 do not match with experimental data on the trend of the curve as well as the values, even though this is the best result that Debye's model can provide using the methodology in this thesis. The curve of loss factor with frequency from Debye's model for oven-dried CP35 increases first and then decreases. This trend is not consistent with the descending trend of experimental results. This is due to mathematical expression shown in Eq. 4-4 which is the expression of the imaginary part of Eq. 4-2. The denominator in right hand side of Eq. 4-4 decreases first as a function of ω, and then increases after the ω is equal to 2.27 GHz which can make $\frac{1}{\omega \times \tau}$ equal to $\omega \times \tau$. Therefore $\epsilon''(\omega)$ increases first when ω is less than 2.27 GHz and the decreases when

ω is greater than 2.27 GHz for oven-dried CP35.

$$\epsilon''(\omega) = \frac{\epsilon_s - \epsilon_\infty}{\frac{1}{\omega \times \tau} + \omega \times \tau} \tag{4.4}$$

where,

$\epsilon''(\omega)$ = Loss factor from modeling at a certain frequency

ϵ_∞ = Dielectric constant at frequency of infinity

ϵ_s = Dielectric constant at frequency of zero

ω = Frequency (GHz)

τ = Relaxation time (ns)

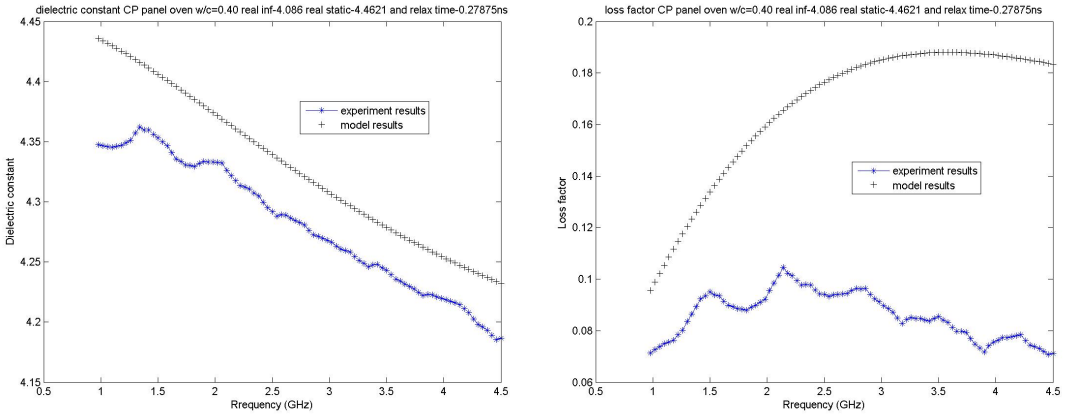

Figure 4-5: Results of dielectric properties for oven-dried CP40 from Debye's model

Figure 4-5 to Figure 4-9 show the results from Debye's model on oven-dried CP40, CP42, CP45, CP50 and CP55, respectively. Dielectric constant from Debye's model can provide results which are close to experimental results with small norm error. However, the error between modeling results and experimental results is mainly from loss

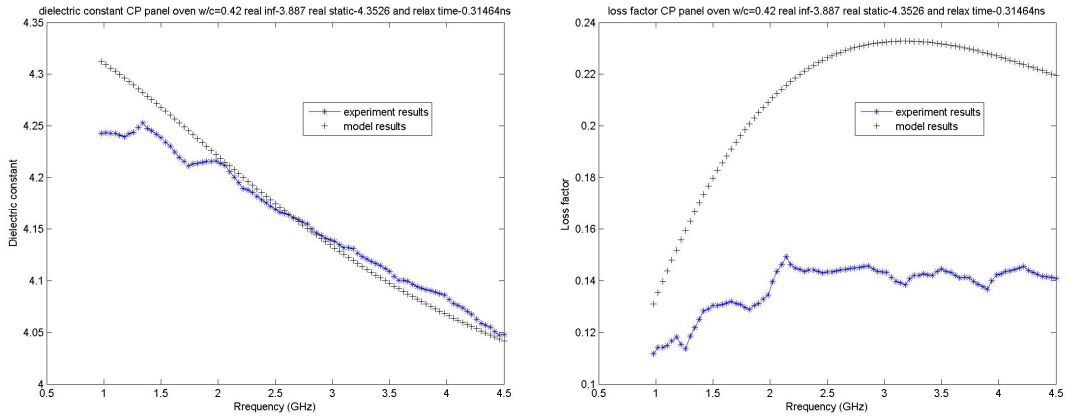

Figure 4-6: Results of dielectric properties for oven-dried CP42 from Debye's model

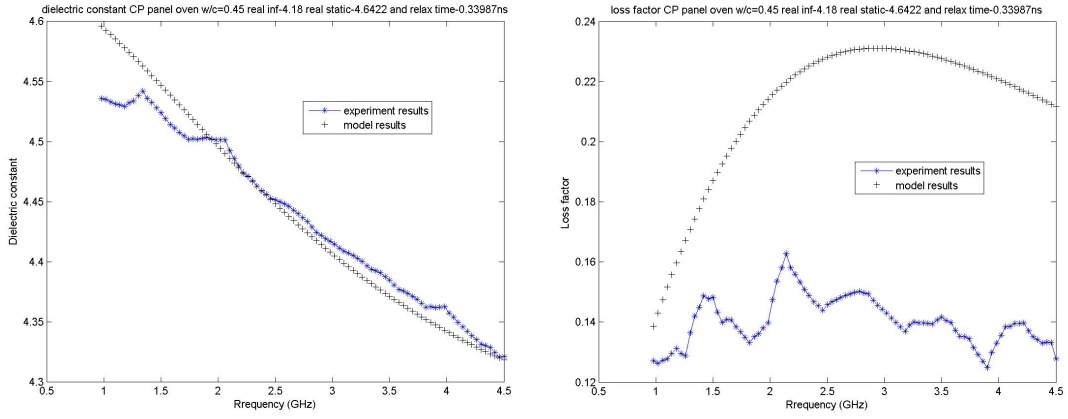

Figure 4-7: Results of dielectric properties for oven-dried CP45 from Debye's model

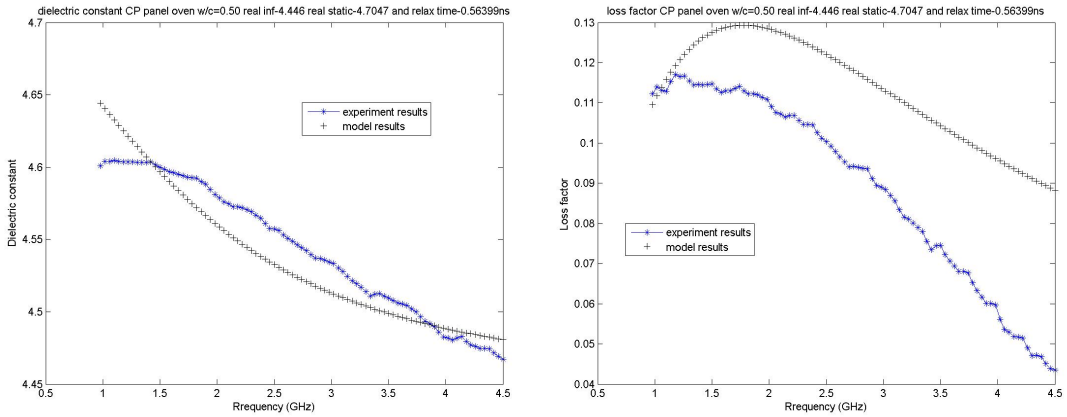

Figure 4-8: Results of dielectric properties for oven-dried CP50 from Debye's model

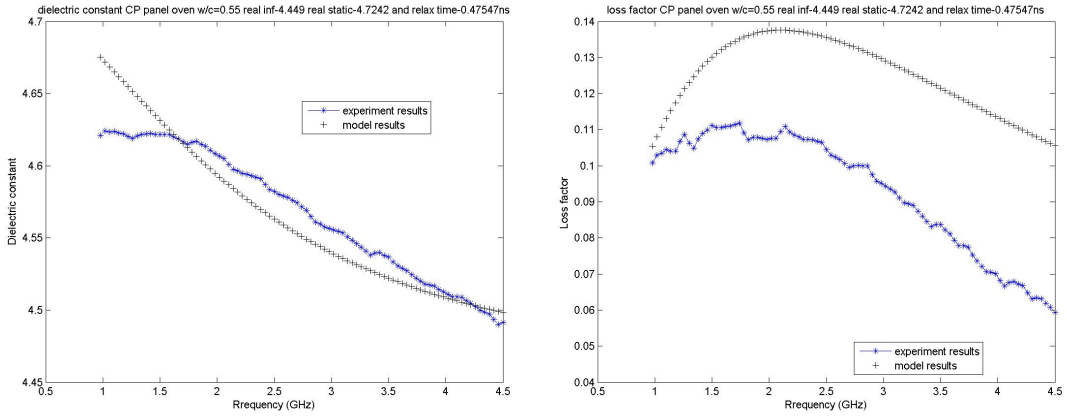

Figure 4-9: Results of dielectric properties for oven-dried CP55 from Debye's model

factor and loss factor does not match with experimental results, which is as the same as the observation from oven-dried CP35.

Table 4.1: Debye's parameters for oven-dried cement paste panels

Description	ϵ_∞	ϵ_s	τ (ns)	NE
CP35	4.035	4.2929	0.4408	0.9970
CP40	4.086	4.4621	0.2788	1.2626
CP42	3.887	4.3526	0.3146	0.9399
CP45	4.180	4.6422	0.3399	0.8920
CP50	4.446	4.7047	0.5640	0.4189
CP55	4.449	4.7242	0.4755	0.4859

Table 4.1 shows Debye's parameters from oven-dried cement paste panels. We can see that ϵ_∞ and ϵ_s increase with the increase of w/c ratio in general, but τ does not have obvious trend.

In summary, dielectric constant from Debye's model is close to experimental data. Nevertheless, loss factor from Debye's model does not match with the results from measurements.

4.1.3 Results of Debye's Model on Room-conditioned Cement Paste Panels

Debye's model is also applied on room-conditioned cement paste panels using the same methodology. Figure 4-10 to Figure 4-15 show the results on room-conditioned CP35, CP40, CP42, CP45, CP50 and CP55, respectively. We have similar observations as the results from oven-dried cement paste panels. Dielectric constant from Debye's model is close to experimental results, but loss factor does not match with experimental results due to mathematical expression of Debye's model on loss factor.

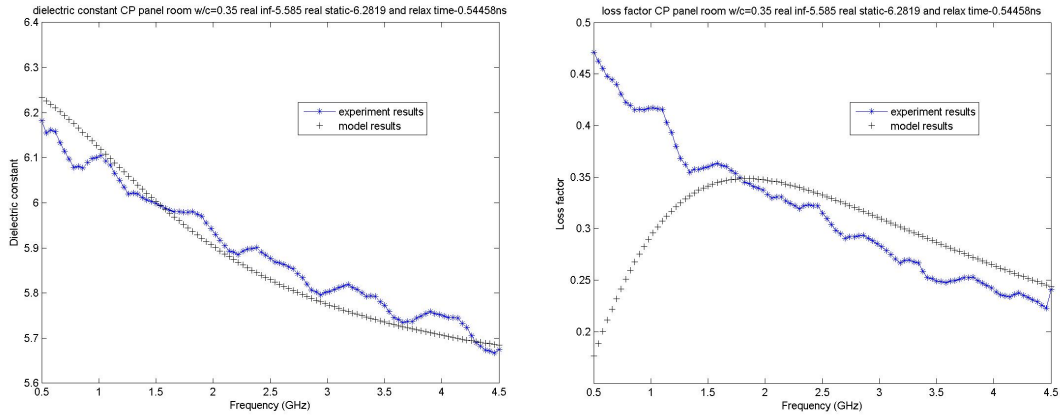

Figure 4-10: Results of dielectric properties for room-conditioned CP35 from Debye's model

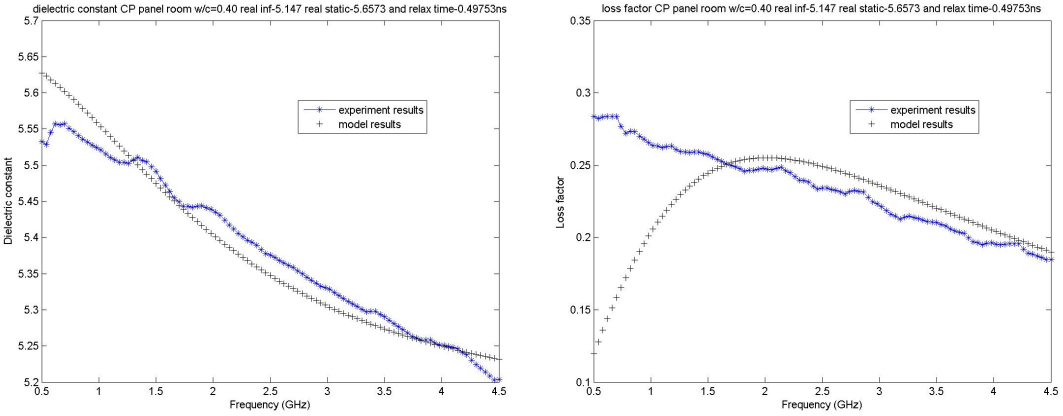

Figure 4-11: Results of dielectric properties for room-conditioned CP40 from Debye's model

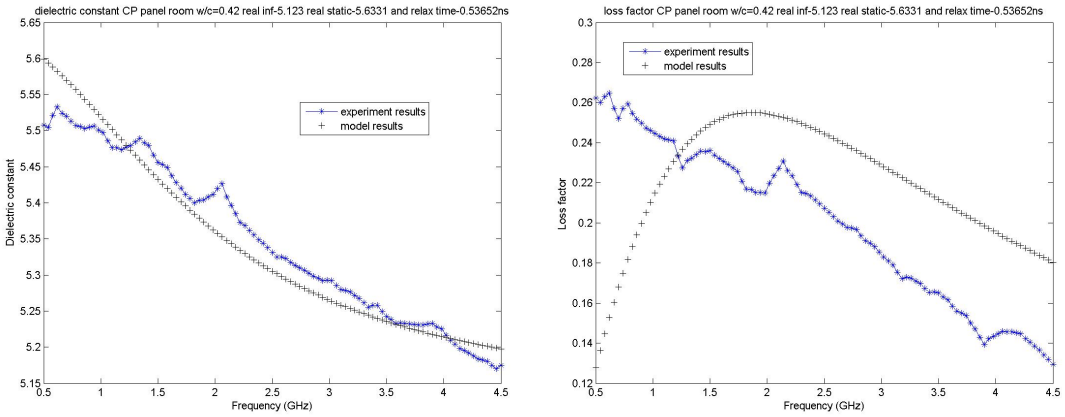

Figure 4-12: Results of dielectric properties for room-conditioned CP42 from Debye's model

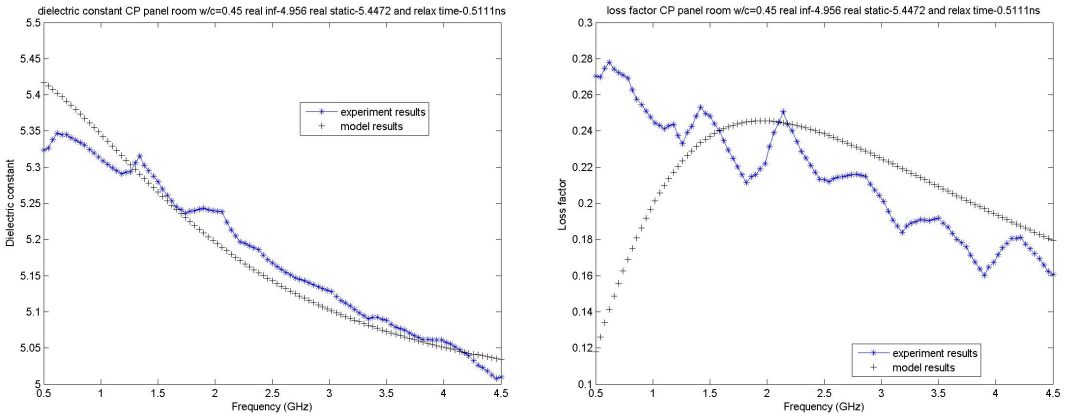

Figure 4-13: Results of dielectric properties for room-conditioned CP45 from Debye's model

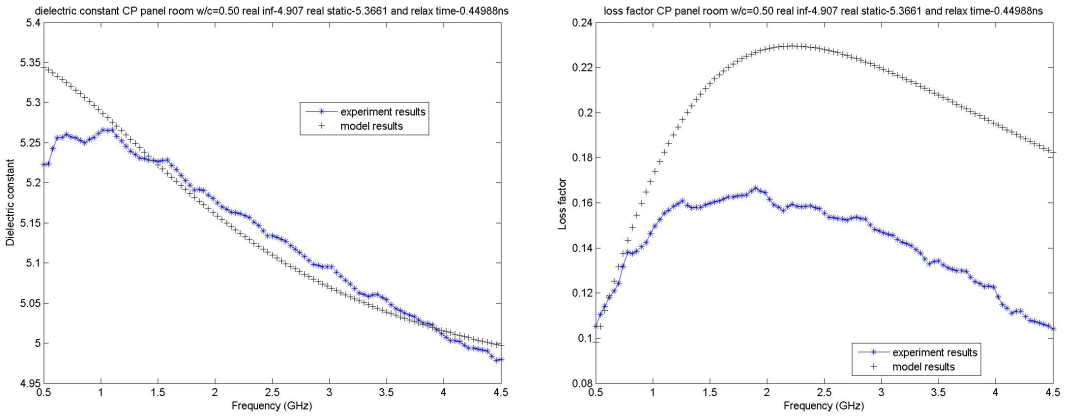

Figure 4-14: Results of dielectric properties for room-conditioned CP50 from Debye's model

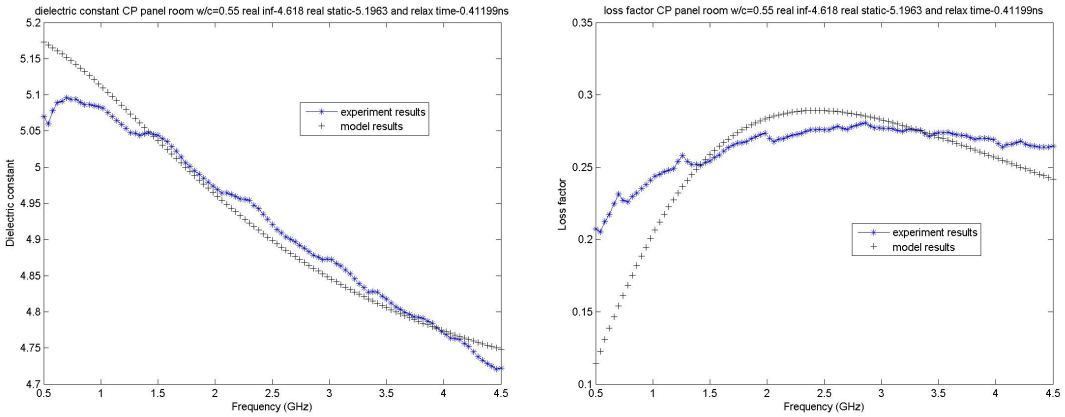

Figure 4-15: Results of dielectric properties for room-conditioned CP55 from Debye's model

Table 4.2: Debye's parameters for room-conditioned cement paste panels

Description	ϵ_∞	ϵ_s	τ (ns)	NE
CP35	5.585	6.2819	0.5446	1.2110
CP40	5.147	5.6573	0.4975	0.7390
CP42	5.123	5.6331	0.5365	0.8066
CP45	4.956	5.4472	0.5111	0.7316
CP50	4.907	5.3661	0.4499	0.9475
CP55	4.618	5.1963	0.4120	0.5622

Table 4.2 shows Debye's parameter on room-conditioned cement paste panels. We can see that ϵ_∞ and ϵ_s show decreased trend with the increase of w/c ratio, which is contrast with the results from oven-dried cement paste panels. In addition, τ for room-conditioned cement paste panels decreases with the increase of w/c ratio in general.

4.2 Havriliak-Negami's Model

4.2.1 Approach of Havriliak-Negami's Model

Havriliak-Negami's (H-N's) model is one improved version of Debye's model which can also be used for materials with non-Debye-type relaxations. The equation of H-N's model is shown in Eq. 4-5. Comparing with Debye's model, there two more parameters in H-N's model, α_2 and γ. These two parameters are both within the range of [0,1] from experience.

$$\epsilon(\omega) = \epsilon_\infty + \frac{\epsilon_s - \epsilon_\infty}{(1 + (i \times \omega \times \tau)^{\alpha_2})^\gamma} \tag{4.5}$$

where,

$\epsilon(\omega)$ = Dielectric properties from modeling

ϵ_∞ = Dielectric constant at frequency of infinity

ϵ_s = Dielectric constant at frequency of zero

i = Symbol of imaginary number

ω = Frequency (GHz)

τ = Relaxation time (ns)

α_2 and γ : Empirical parameters.

Figure 4-16 shows the process of H-N's model. The method to determine ϵ_∞ is as the same as Debye's model. The following part is also similar with Debye's model. The difference is that H-N's model has two more parameters to assume within their possible ranges. By plugging assumed values into Eq. 4-5, the final determined values of ϵ_s, τ, α_2 and γ are also from the combination which can lead to the smallest NE from both dielectric constant and loss factor between modeling results and experimental results.

4.2.2 Results of Havriliak-Negami's on Oven-dried Cement Paste Panels

Since the process to determine ϵ_∞ is as the same as Debye's model, we will get the same ϵ_∞ for oven-dried cement paste panels with each w/c ratio. However, since there are two additional parameters in H-N's model, different values of ϵ_s, τ, α_2 and γ may be obtained. As well, we will probably get different modeling results of dielectric properties.

Figure 4-17 to Figure 4-22 show the results from H-N's model. We can see that the performance of H-N's model on loss factor is better than Debye's model from smaller

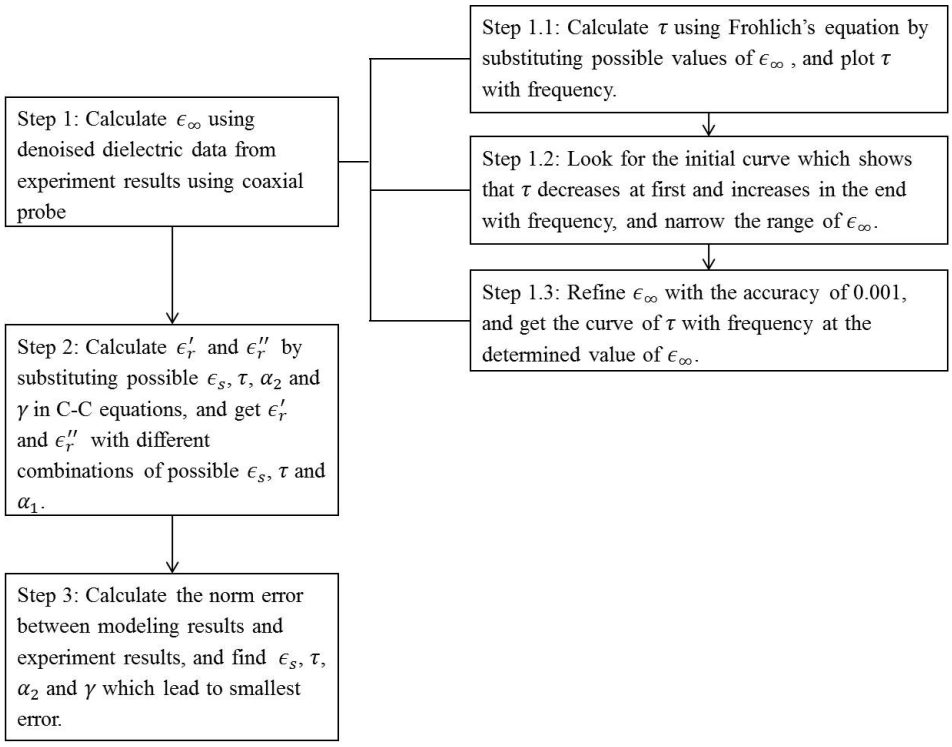

Figure 4-16: Process of Havriliak-Negami's model

NE, even though the curves of loss factor from H-N's model still cannot fit the experimental results. In addition, the results of dielectric constant from Debye's model and H-N's model are similar except CP35.

Table 4.3 shows the parameters obtained from H-N's model. From the values of NE, H-N's model gives better results than Debye's model in the view of difference between modeling and experiments. The change of α_2 and γ is the main reason leading to the better results since α_2 and γ are fixed in Debye's model actually. On the other hand, ϵ_∞ and ϵ_s from H-N's model are the same as those from Debye's model. However, τ is changed for CP42, CP45, CP50, and CP55. This is also because of the change of α_2 and γ such that the combination of these four parameters which can lead to the final results is changed.

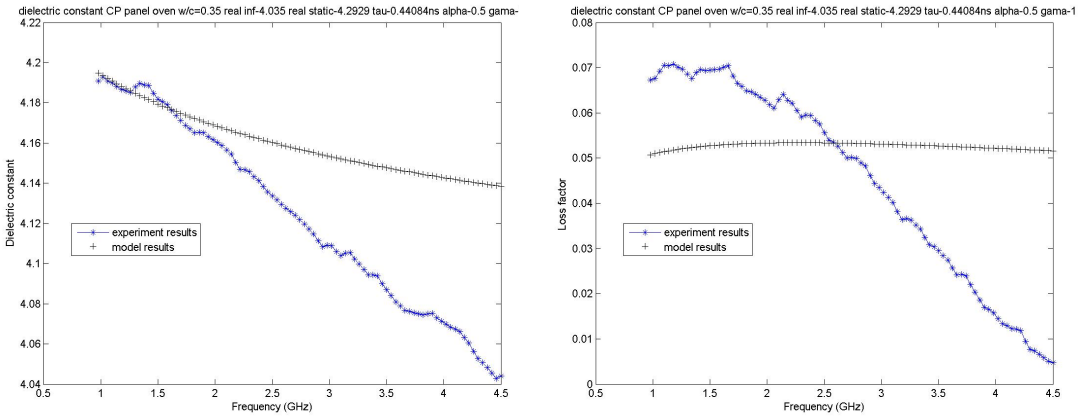

Figure 4-17: Results of dielectric properties for oven-dried CP35 from H-N's model

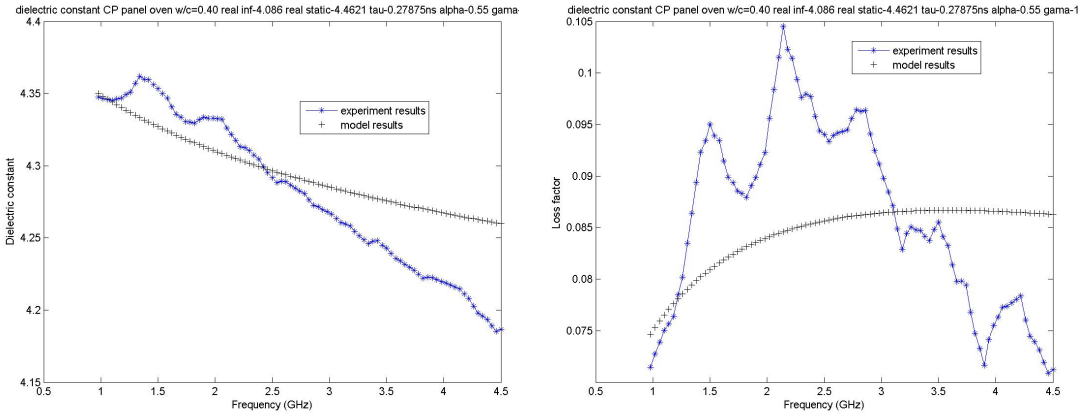

Figure 4-18: Results of dielectric properties for oven-dried CP40 from H-N's model

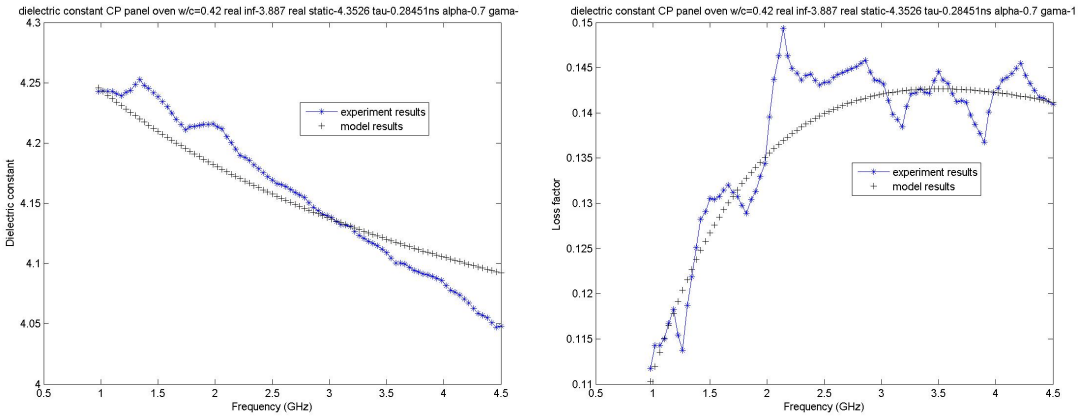

Figure 4-19: Results of dielectric properties for oven-dried CP42 from H-N's model

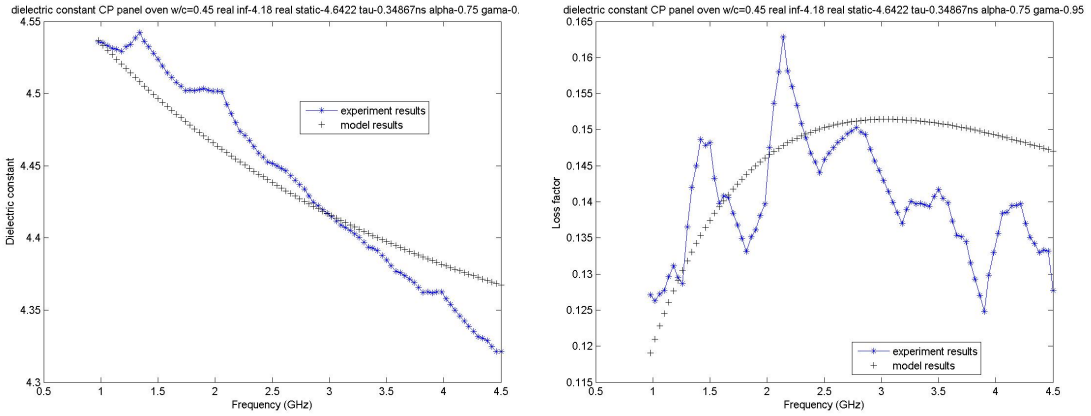

Figure 4-20: Results of dielectric properties for oven-dried CP45 from H-N's model

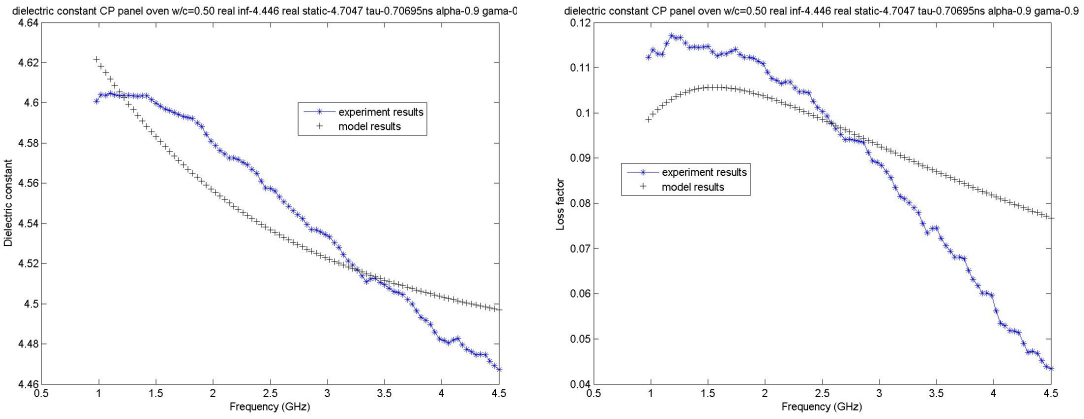

Figure 4-21: Results of dielectric properties for oven-dried CP50 from H-N's model

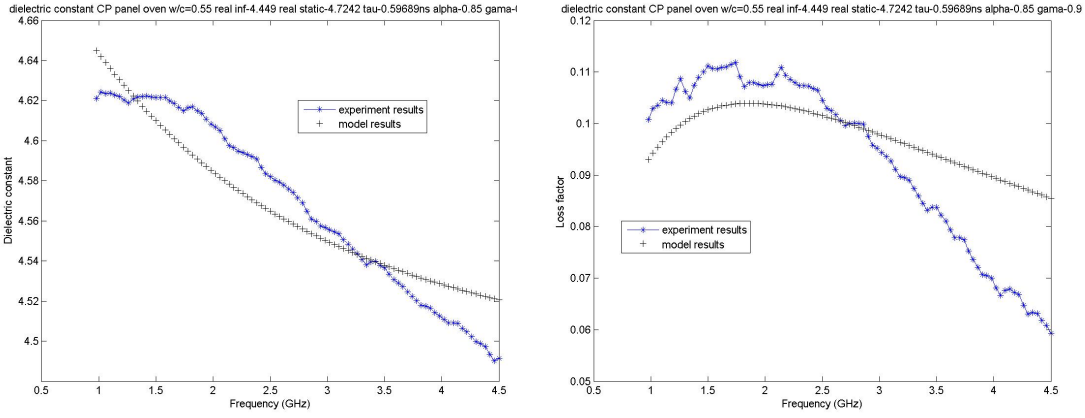

Figure 4-22: Results of dielectric properties for oven-dried CP55 from H-N's model

Table 4.3: H-N's parameters for oven-dried cement paste panels

Description	ϵ_∞	ϵ_s	τ (ns)	α_2	γ	NE
CP35	4.035	4.2929	0.4408	0.5	1	0.6675
CP40	4.086	4.4621	0.2788	0.55	1	0.3947
CP42	3.887	4.3526	0.2845	0.7	1	0.2364
CP45	4.180	4.6422	0.3487	0.75	0.85	0.3161
CP50	4.446	4.7047	0.7070	0.9	0.9	0.3084
CP55	4.449	4.7242	0.5967	0.85	0.9	0.2620

4.2.3 Results of Havriliak-Negami's on Room-conditioned Cement Paste Panels

H-N's model is also performed on room-conditioned cement paste panels. Figure 4-23 to Figure 4-28 show the modeling results from H-N's model on room-conditioned cement paste panels. We can see that results from H-N's model have good agreement with experimental results on room-conditioned cement paste panels. Comparing with the results from Debye's model, H-N's model improves the performance on loss factor of room-conditioned cement paste panels due to the two additional parameters α_2 and γ. The two parameters α_2 and γ have more influence on loss factor.

Table 4.4 shows the parameters obtained from H-N's model on room-conditioned cement paste panels. From the table, ϵ_s and τ show the general descending trend with the increase of w/c ratio. In addition, α_2 and γ are very stable for room-conditioned cement paste panels.

Comparing with Debye's parameters on room-conditioned cement paste panels, ϵ_s and τ are changed except CP55 due to the change of α_2 and γ. Also, NE is reduced because of better performance of H-N's model on room-conditioned cement paste panels.

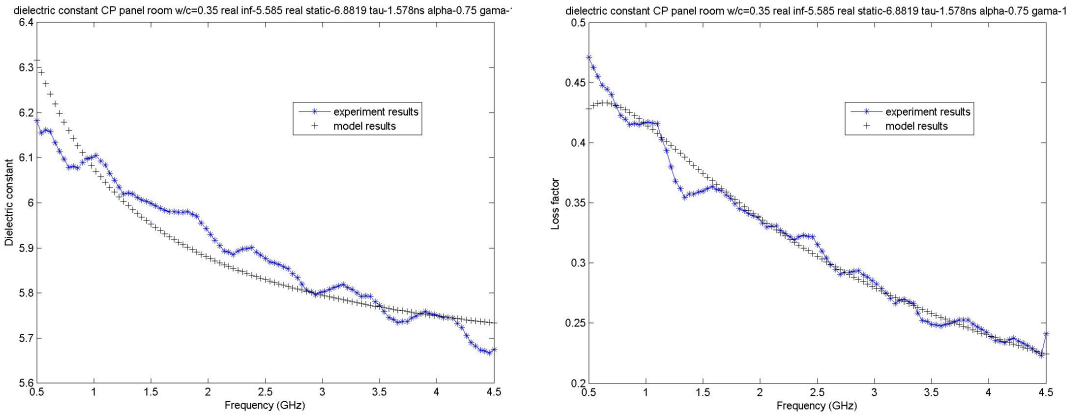

Figure 4-23: Results of dielectric properties for room-conditioned CP35 from H-N's model

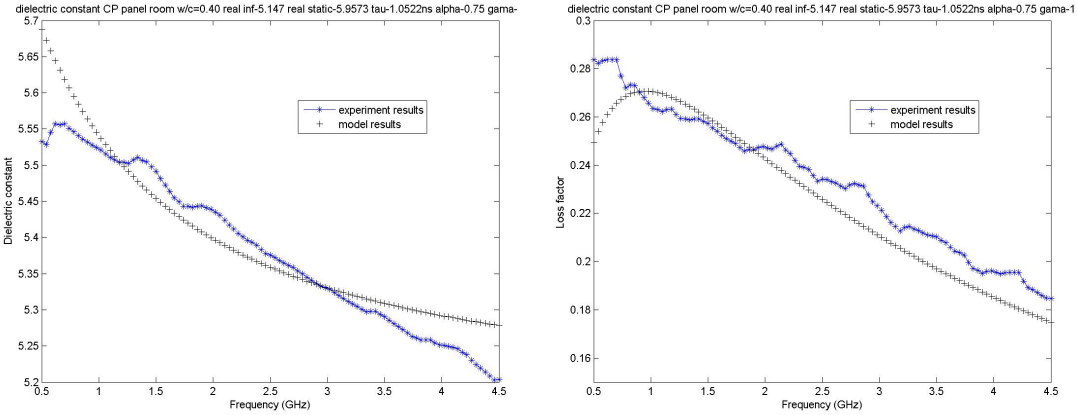

Figure 4-24: Results of dielectric properties for room-conditioned CP40 from H-N's model

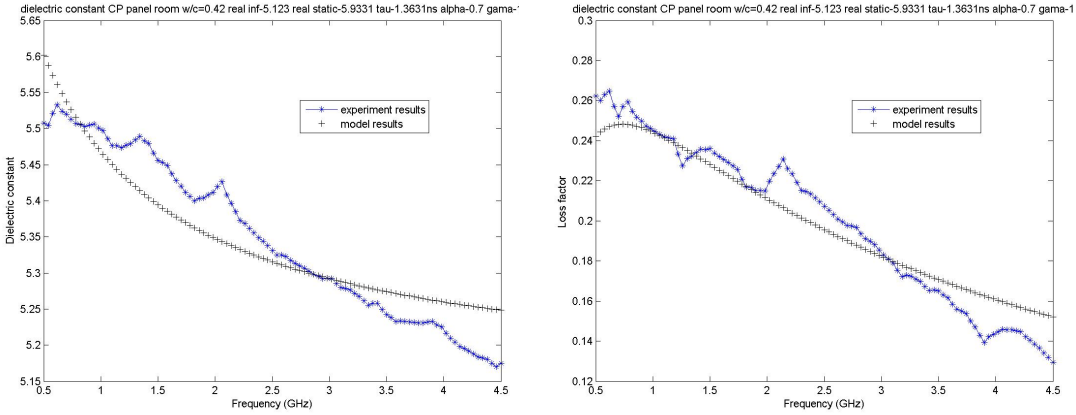

Figure 4-25: Results of dielectric properties for room-conditioned CP42 from H-N's model

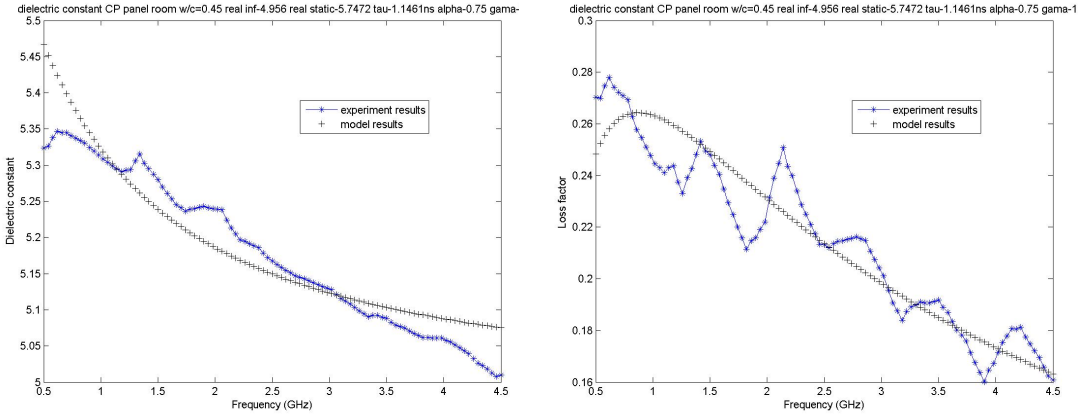

Figure 4-26: Results of dielectric properties for room-conditioned CP45 from H-N's model

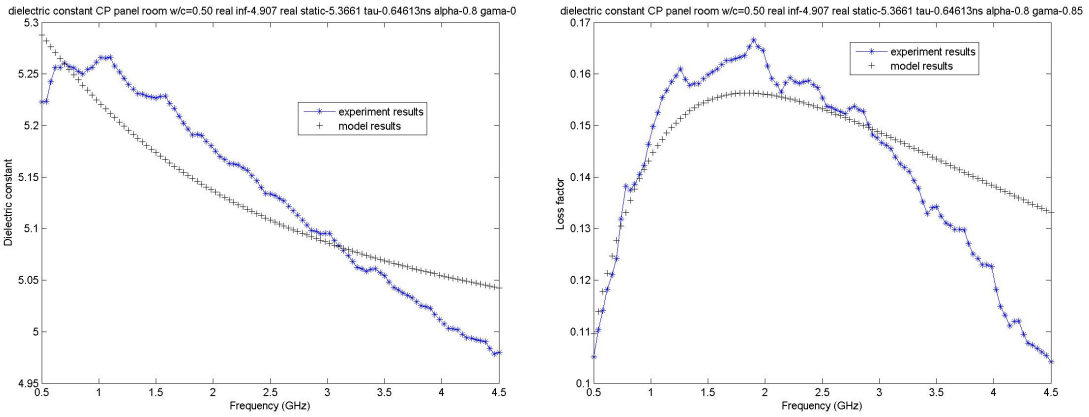

Figure 4-27: Results of dielectric properties for room-conditioned CP50 from H-N's model

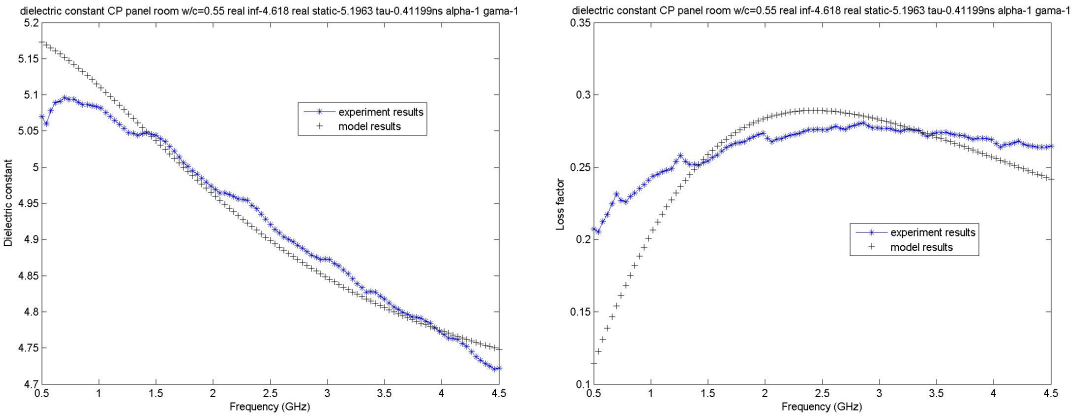

Figure 4-28: Results of dielectric properties for room-conditioned CP55 from H-N's model

Table 4.4: H-N's parameters for room-conditioned cement paste panels

Description	ϵ_∞	ϵ_s	τ (ns)	α_2	γ	NE
CP35	5.585	6.8819	1.578	0.75	1	0.5815
CP40	5.147	5.9573	1.052	0.75	1	0.5262
CP42	5.123	5.9331	1.363	0.7	1	0.5568
CP45	4.956	5.7472	1.146	0.75	1	0.5115
CP50	4.907	5.3661	0.646	0.8	0.85	0.4933
CP55	4.618	5.1963	0.412	1	1	0.5622

4.3 Yu's Model on Oven-dried Cement Paste Panels

4.3.1 Approach of Yu's Model

Since Debye's model and H-N's model cannot provide good agreement with experimental results on loss factor of oven-dried cement paste panels, Yu's model is used for improving modeling results. Yu's model is a modified Debye's model for oven-dried cement paste panels by involving w/c ratio which is the specific parameter of cementitious material [30]. Eq. 4-6 shows the mathematical expression of Yu's model.

$$\epsilon(\omega) = \epsilon_\infty + \frac{\epsilon_s - \epsilon_\infty}{1 + (i \times \omega \times \tau)^{\alpha \times \Psi}} = \frac{\gamma}{(C_1 + \Psi) \times C_2} + \frac{\frac{\gamma}{(C_3+\Psi)\times C_4}}{1 + (i \times \omega \times \tau)^{\alpha \times \Psi}} \tag{4.6}$$

where,

$\epsilon(\omega)$ = Dielectric properties from Yu's model

ϵ_∞ = Dielectric constant at frequency of infinity

ϵ_s = Dielectric constant at frequency of zero

i = Symbol of imaginary number

ω = Frequency (GHz)

τ = Relaxation time (ns)

Ψ = W/c ratio

C_1, C_2, C_3, C_4, γ and α : Parameters determined by experiment.

Figure 4-29 show the process of Yu's model. C_1, C_2, C_3, C_4 and γ are determined first by the ϵ_∞ and ϵ_s obtained from Debye's model and H-N's model. After that, plug assumed possible α and τ into Eq. 4-6 and calculate dielectric properties from different combinations of α and τ. It is assumed that α is within the range [0,1] with the increment of 0.05, and that τ are based on that from Debye's model and H-N's model. Finally, α and τ are determined by the combination which can lead to the smallest NE between modeling results and experimental results.

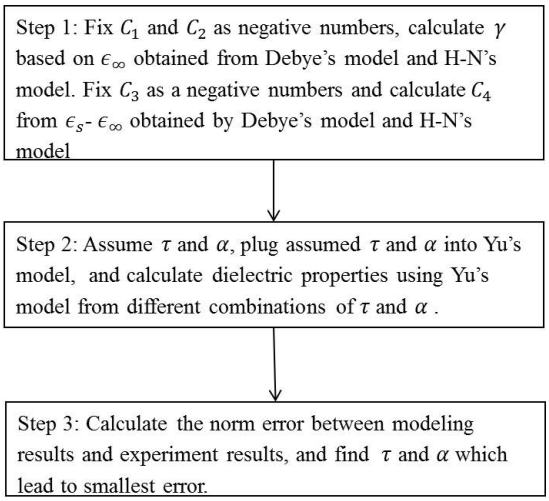

Figure 4-29: Process of Yu's model

4.3.2 Results of Yu's Model on Oven-dried Cement Paste Panels

Table 4.5 shows Yu's parameters. The parameter NE indicates that Yu's model provides better overall results of dielectric properties on oven-dried cement paste panels for each w/c ratio due to smaller NE. In addition, C_4 shows descending trend with the increase of w/c ratio except oven-dried CP35, and the value of $\alpha \times \psi$ increases with w/c ratio.

Figure 4-30 to Figure 4-35 shows the final results from Yu's model. Yu's model has better overall performance on dielectric properties of oven-dried cement paste panels, especially on loss factor part.

Table 4.5: Yu's parameters for oven-dried cement paste panels

Description	C_1	C_2	C_3	C_4	γ	τ (ns)	$\alpha \times \Psi$	NE
CP35	-1.25	-0.4	-1	-8.7370	1.4533	1.1545	0.57	0.4755
CP40	-1.25	-0.4	-1	-6.4354	1.3943	0.4297	0.60	0.3422
CP42	-1.25	-0.4	-1	-5.6738	1.3137	0.3916	0.80	0.2277
CP45	-1.25	-0.4	-1	-6.2700	1.3594	0.4209	0.82	0.2630
CP50	-1.25	-0.4	-1	-10.705	1.3365	0.6497	0.90	0.3006
CP55	-1.25	-0.4	-1	-11.034	1.2522	0.5445	0.90	0.2474

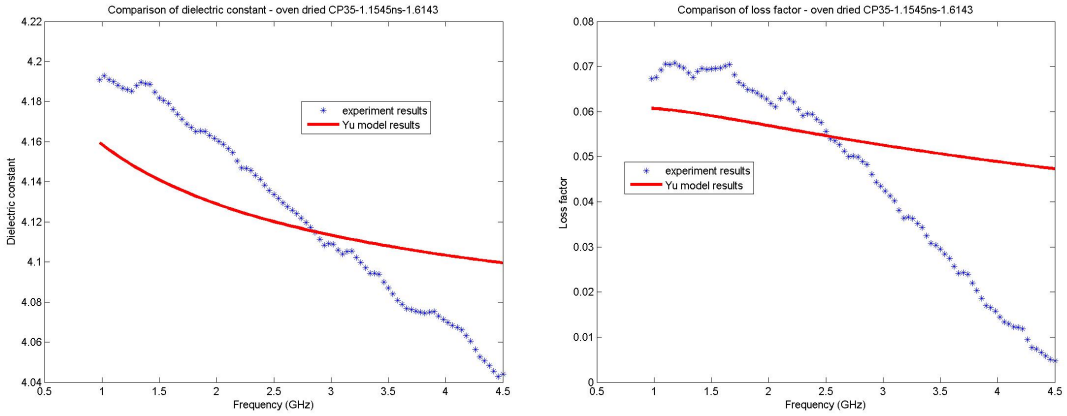

Figure 4-30: Results of dielectric properties for oven-dried CP35 from Yu's model

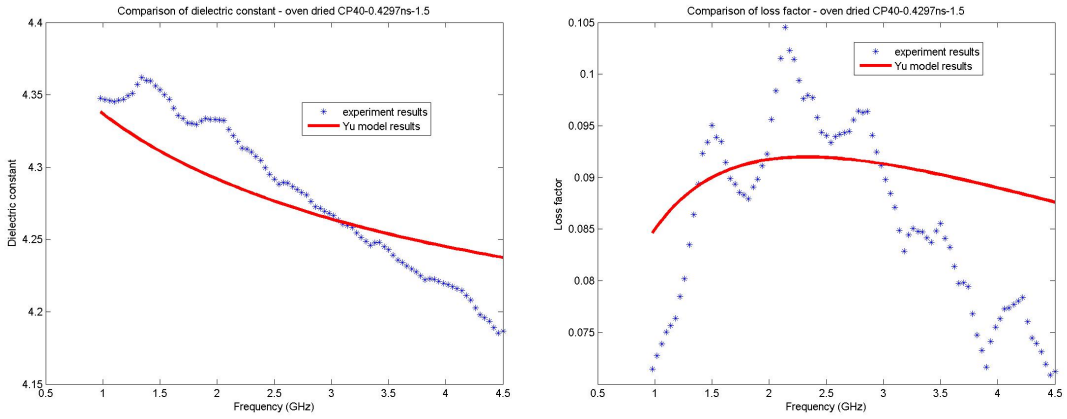

Figure 4-31: Results of dielectric properties for oven-dried CP40 from Yu's model

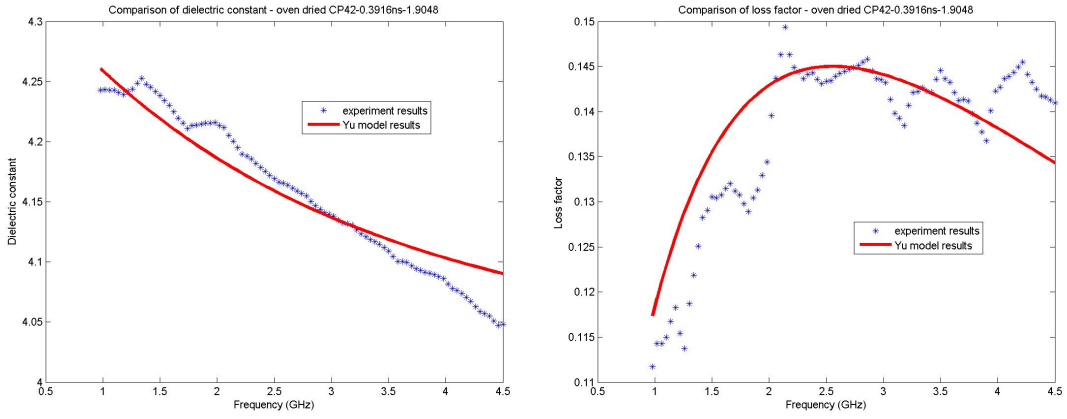

Figure 4-32: Results of dielectric properties for oven-dried CP42 from Yu's model

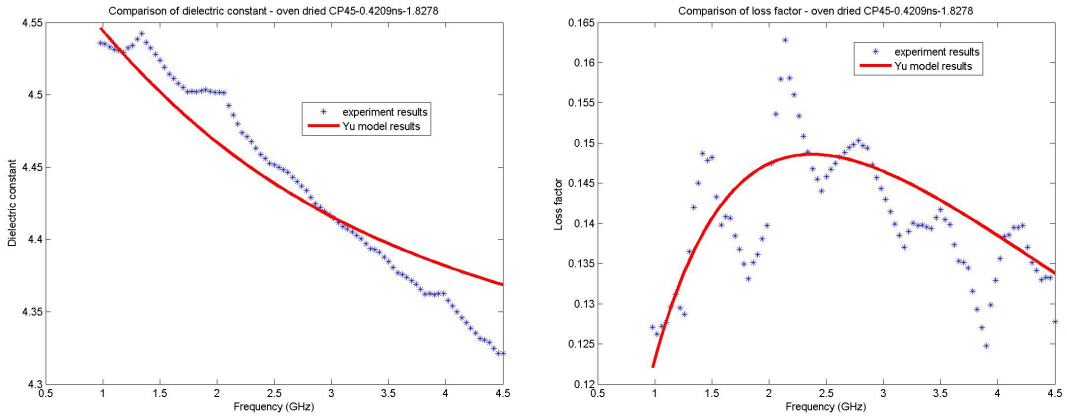

Figure 4-33: Results of dielectric properties for oven-dried CP45 from Yu's model

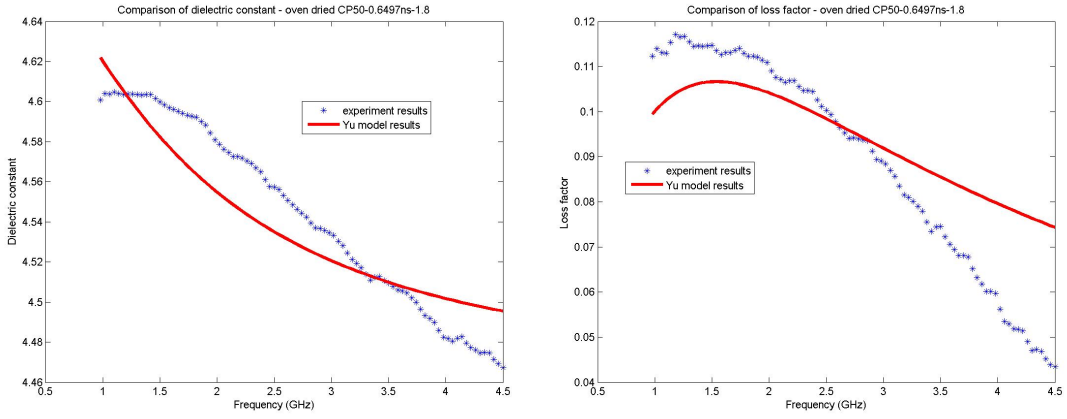

Figure 4-34: Results of dielectric properties for oven-dried CP50 from Yu's model

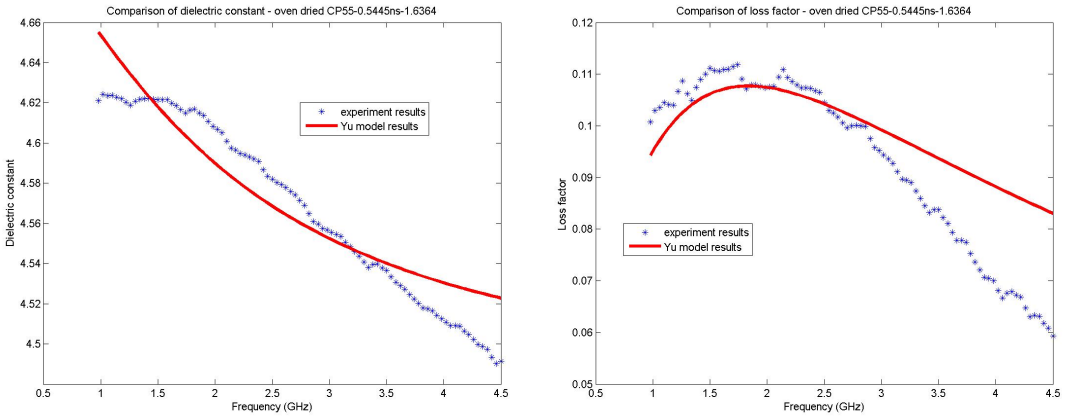

Figure 4-35: Results of dielectric properties for oven-dried CP55 from Yu's model

4.3.3 Comparison of Different Models on Oven-dried Cement Paste Panels

Three models are used for modeling dielectric properties on oven-dried cement paste panels. These three models can provide good agreement with experimental results on dielectric constant part. But loss factor from modeling does not match experimental results, even though Yu's model can have the best performance on loss factor of oven-dried cement paste panels in these three models.

In order to show that Yu's model has the best performance on oven-dried cement paste panels among these three models, percentage error (*PE*) analysis is performed. The equations of *PE* for dielectric constant and loss factor are shown in Eq. 4-7 and Eq. 4-8, respectively.

$$PE'(\omega) = 100\% \times \frac{\epsilon'_m(\omega) - \epsilon'_{exp}(\omega)}{\epsilon'_{exp}(\omega)} \tag{4.7}$$

$$PE''(\omega) = 100\% \times \frac{\epsilon_m''(\omega) - \epsilon_{exp}''(\omega)}{\epsilon_{exp}''(\omega)} \tag{4.8}$$

where,

$PE'(\omega)$ = Percentage error of dielectric constant

$PE''(\omega)$ = Percentage error of loss factor

$\epsilon_m'(\omega)$ = Dielectric constant from modeling at a certain frequency

$\epsilon_{exp}'(\omega)$ = Dielectric constant from experimental measurements at a certain frequency

$\epsilon_m''(\omega)$ = Loss factor from modeling at a certain frequency

$\epsilon_{exp}''(\omega)$ = Loss factor from experimental measurements at a certain frequency

Figure 4-36 to Figure 4-41 show the comparison of PE from different models on oven-dried cement paste panels for each w/c ratio. For dielectric constant, the PE for Debye's model, H-N's model and Yu's model is lower than ±3%. For loss factor, the PE from Debye's model is very large, but H-N's model and Yu's model provide less PE. Yu's model has slightly better performance on loss factor than H-N's model in overall view. However, neither of these models have good results on oven-dried CP35.

4.4 Summary

In this chapter, three models, Debye's model, H-N's model, and Yu's model, are introduced and these three models are applied on oven-dried and room-conditioned cement paste panels.

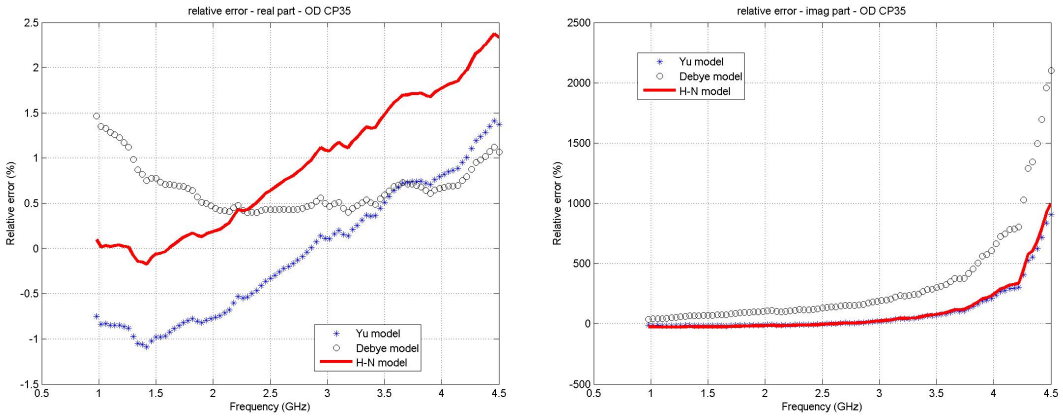

Figure 4-36: Comparison of *PE* from different models for oven-dried CP35

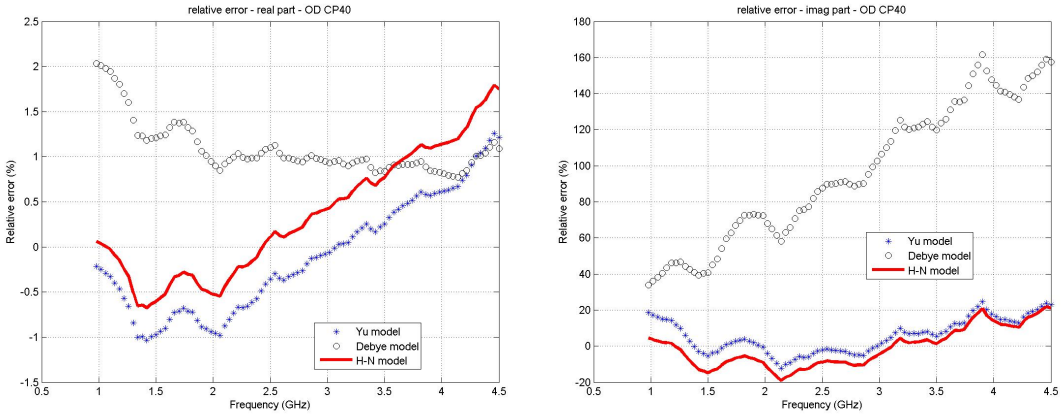

Figure 4-37: Comparison of *PE* from different models for oven-dried CP40

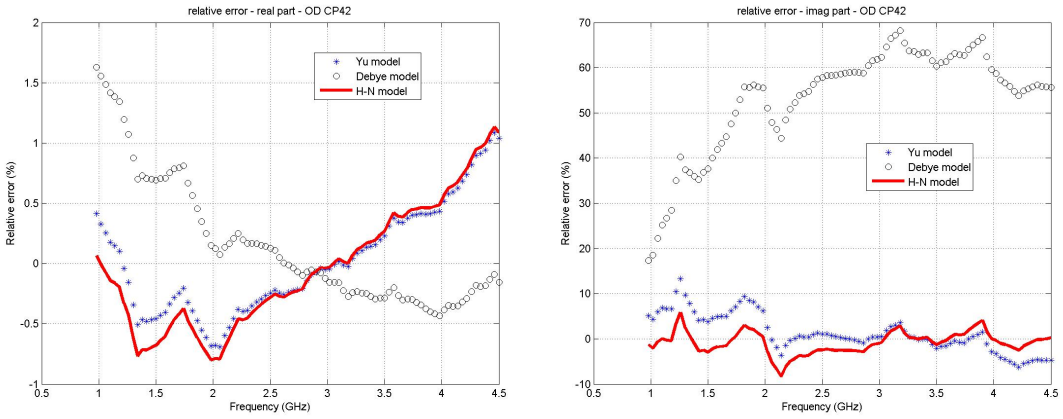

Figure 4-38: Comparison of *PE* from different models for oven-dried CP42

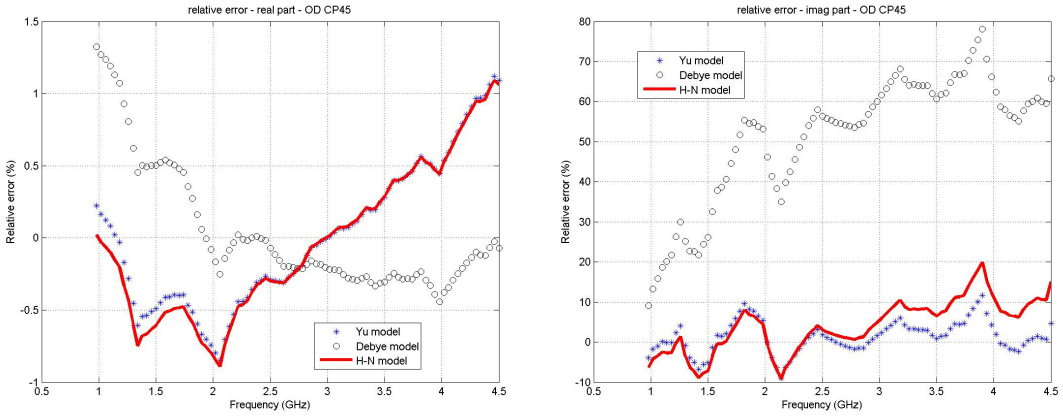

Figure 4-39: Comparison of *PE* from different models for oven-dried CP45

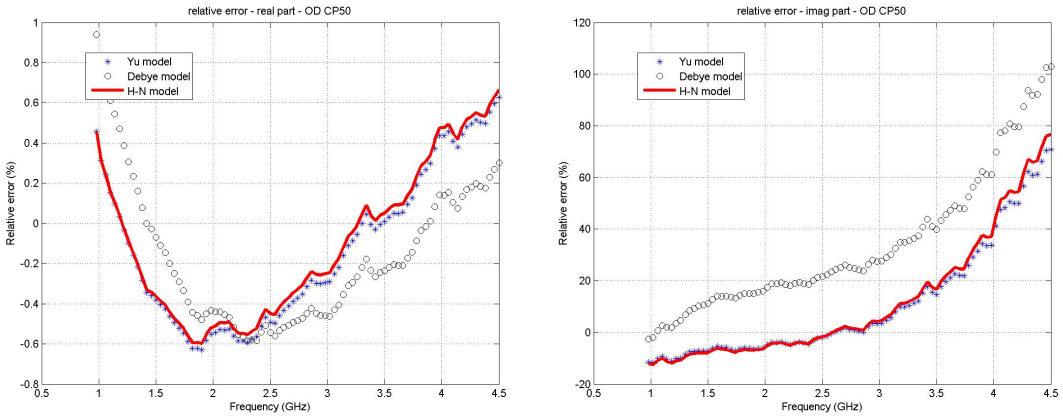

Figure 4-40: Comparison of *PE* from different models for oven-dried CP50

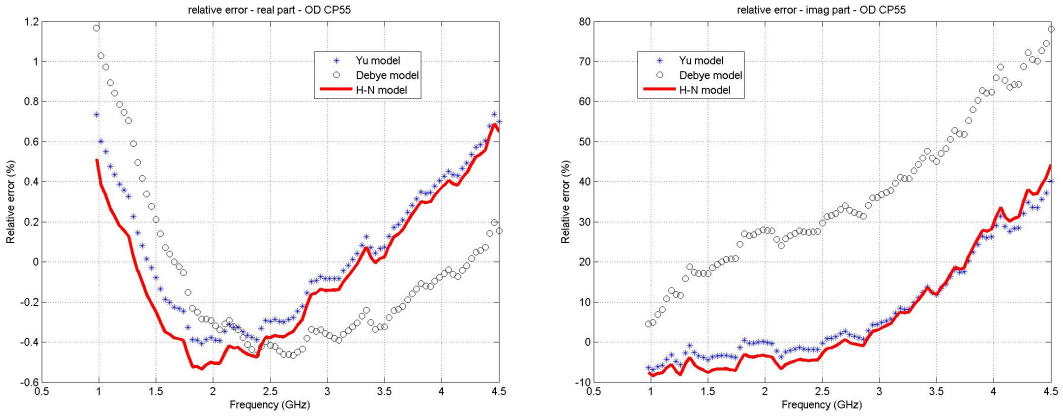

Figure 4-41: Comparison of *PE* from different models for oven-dried CP55

For the performance on oven-dried cement paste panels, we can summarize our observations in the following:

- Yu's model can provide best overall performance among these three models on oven-dried cement paste panels. The performance of H-N's model is close to Yu's model.

- These three models can provide small *PE* on dielectric constant, but relatively large *PE* on loss factor. Debye's model does not work on loss factor due to large *PE*, nevertheless H-N's model and Yu's model provide better results on loss factor even though the results still do not match with experimental results totally.

- The common parameters for Debye's model and H-N's model, ϵ_∞ and ϵ_s increases with the increase of w/c ratio in general. On the other hand, α from H-N's model increases with w/c ratio generally, but γ is very stable for each w/c ratio.

For the performance on room-conditioned cement paste panels, the observations can be summarized in the following:

- The results from H-N's model have good agreement with experimental results on both dielectric constant and loss factor. Debye's model can provide similar results on dielectric constant but not good results on loss factor. This is due to two extra parameters that H-N's model has.

- The common parameters for Debye's model and H-N's model, ϵ_∞ and ϵ_s decreases with the increase of w/c ratio. On the other hand, α from H-N's model

increases with w/c ratio, but γ is very stable for each w/c ratio.

Chapter 5

Results of Heterogeneous Dielectric Models on Cement Paste Panels

In this chapter, heterogeneous dielectric models are used for modeling dielectric properties of cement paste panels. The models used in this chapter include Maxwell-Garnett's model, Wiener's model and Polder-van Santen's model. In this chapter, the host material is always hydrated cement since the coaxial probe contacts directly with hydrated cement during experimental measurements. The inclusion material in oven-dried cement paste panels is air, and the inclusion materials in room-conditioned cement paste panels are air and water. The over-all/effective dielectric properties are the dielectric properties for oven-dried or room-conditioned cement paste panels. The process and results of modeling are introduced, and the validity of these models are verified as well. Maxwell-Garnett's model and Wiener's model are used in the inverse way to calculate the dielectric properties of the host material. After this, the dielectric properties of the host material were plugged into Polder-van Santen's model and see how this model

works on the modeling of the dielectric properties of room-conditioned cement paste panels.

There are several assumptions for these three heterogeneous models: i) The polarizable inclusion is assumed to exist in a homogeneous host material, which means that hydrated cement is assumed to be homogeneous in this thesis. ii) Inclusion materials are assumed to be discrete for all these three models to maintain the same permittivity profiles and neglect the interactions between particles. iii) The dimension of the largest particle must be much less than a wave-length of EM wave such that scattering losses can be neglected. In our case, a wave-length of EM wave is 0.067 mm to 0.6 mm. Therefore the dimension of the largest inclusion is much less than 0.067 mm in our case.

5.1 Maxwell-Garnett's Model

5.1.1 Approach of Maxwell-Garnett's Model

Maxwell-Garnett's (M-G's) is a two-phase model. In our case, room-conditioned cement paste panels are three-phase material including hydrated cement, air and water. Thus M-G's model cannot be used on room-conditioned cement paste panels.

Besides the three assumptions mentioned above, there are two additional assumptions for M-G's model. Maxwell treated the mixing materials as the anisotropic inclusions in an isotropic magnetic medium by neglecting all particle interactions. In addition, the shape of inclusion material is assumed to be sphere. The equation of

M-G's model is shown in Eq. 5-1.

$$\epsilon = \epsilon_h + \frac{3 \times V_i \times \epsilon_h}{\frac{\epsilon_i + 2 \times \epsilon_h}{\epsilon_i - \epsilon_h} - V_i} \tag{5.1}$$

where,

ϵ = Dielectric properties of the mixing material

ϵ_h = Dielectric properties of the host material

ϵ_i = Dielectric properties of the inclusion material

V_i = Volumetric ratio of the inclusion material

From coaxial probe measurements, we can obtain the overall dielectric properties of mixing materials which are oven-dried cement paste panels in our case. Figure 5-1 and Figure 5-2 show the experimental results on dielectric constant and loss factor, respectively. We can see that the dielectric constant increases with the increase of w/c ratio in general, while the loss factor does not have obvious trend. Additionally, we know the dielectric properties of the inclusion material which is air in this case. Also, the volumetric ratio of air is determined experimentally from ASTM C642 "Standard Test Method for Density, Absorption and Voids in Hardened Concrete"[5] and the results for oven-dried cement paste panels are shown in Table 5.1.

By plugging the dielectric properties of the mixing material and the inclusion material and the volumetric ratio of air, the dielectric properties of host material can be calculated in the inverse way of M-G's model. The process of M-G's model is show in Figure 5-3.

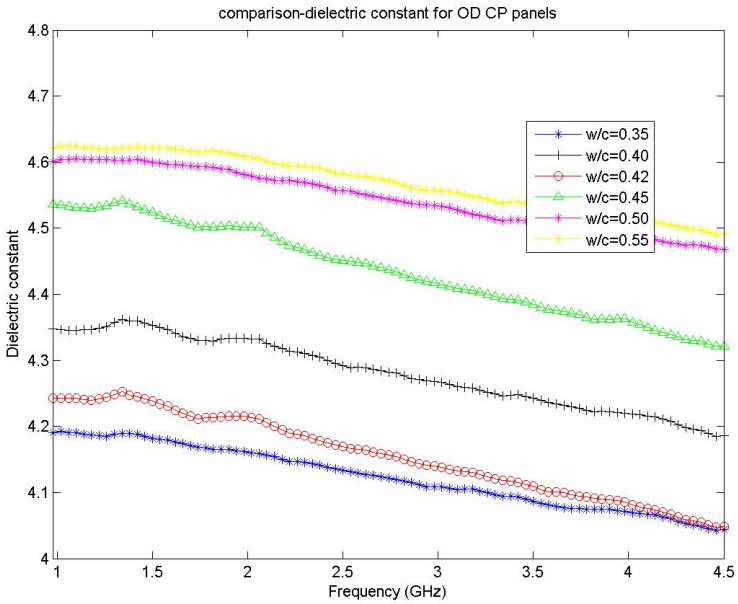

Figure 5-1: Comparison of experimental results on dielectric constant of oven-dried cement paste

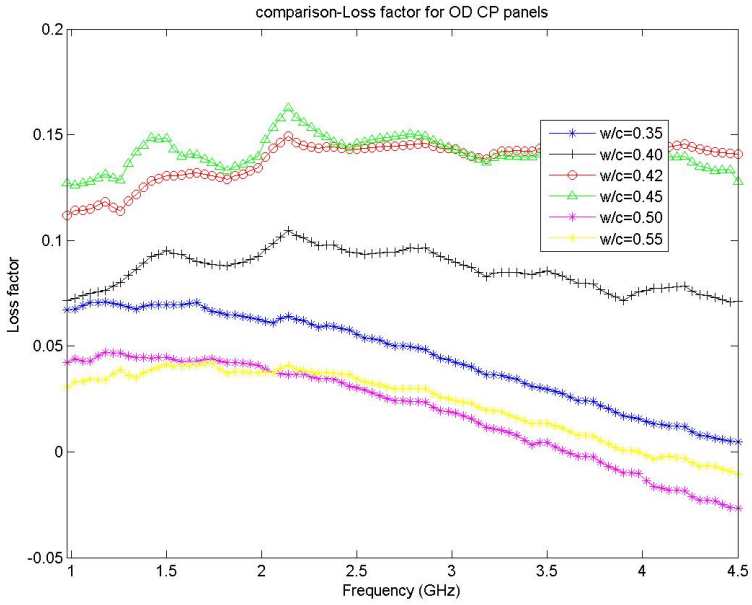

Figure 5-2: Comparison of experimental results on loss factor of oven-dried cement paste

Table 5.1: Volumetric ratio of oven-dried cement paste panels

Sample	Volumetric ratio of air(%)
CP35	40.2
CP40	54.3
CP42	50.4
CP45	57.7
CP50	56.8
CP55	57.0

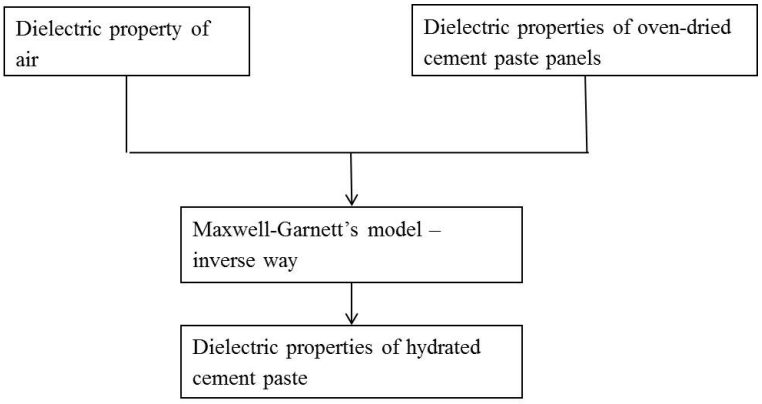

Figure 5-3: Process of M-G's model

5.1.2 Results of Maxwell-Garnett's Model on Oven-dried Cement Paste Panels

Using the approach discussed above, we can calculate the dielectric properties of host material which is hydrated cement with different w/c ratios. The results on oven-dried CP35 are used as examples. Figure 5-4 shows the comparison of dielectric constant on host material which hydrated cement and mixing material which is oven-dried cement paste panel with the w/c ratio of 0.35. As well the comparison of loss factor is shown in Figure 5-5. We can see that the dielectric constant of hydrated cement is larger than that of oven-dried cement paste panels, as well as loss factor. This is because air which is inclusion material has the lowest dielectric constant and loss factor. Therefore

the dielectric properties of hydrated cement have to be higher than overall dielectric properties of mixing material. Also, we have the same observations from the other w/c ratios.

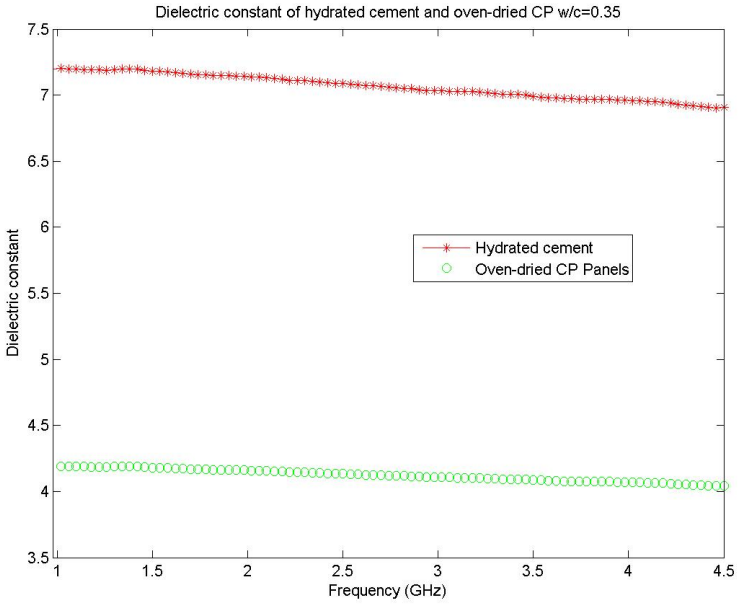

Figure 5-4: Comparison of dielectric constant of hydrated cement and oven-dried cement paste - w/c=0.35

Comparing the dielectric properties of hydrated cement with different w/c ratios, it is found that both the dielectric constant and loss factor have the similar trend with w/c ratio as the results from oven-dried cement paste panels. The comparisons of dielectric constant and loss factor are shown in Figure 5-6 and Figure 5-7, respectively.

5.1.3 Effectiveness of Maxwell-Garnett's Model by Numerical Method

After calculating dielectric properties of host material by the inverse way of M-G's model, one question has been brought up: whether M-G's model is effective in calcu-

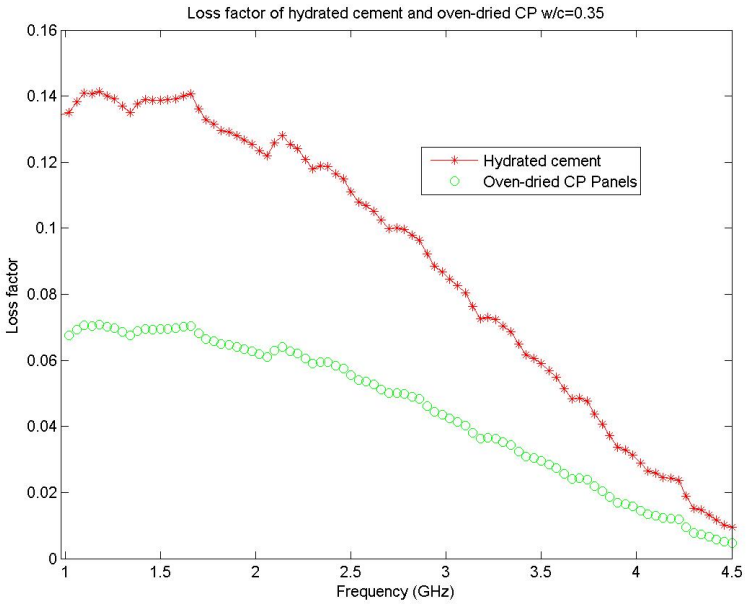

Figure 5-5: Comparison of loss factor of hydrated cement and oven-dried cement paste - w/c=0.35

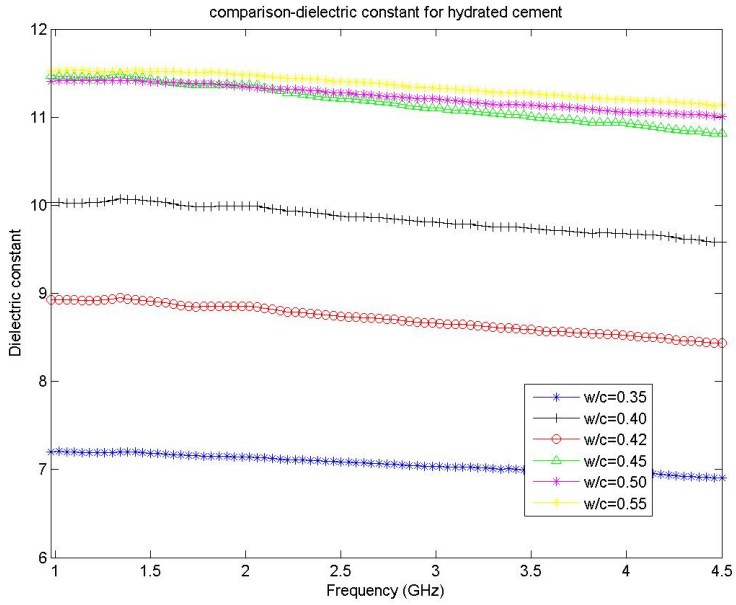

Figure 5-6: Comparison of dielectric constant of hydrated cement with different w/c ratios

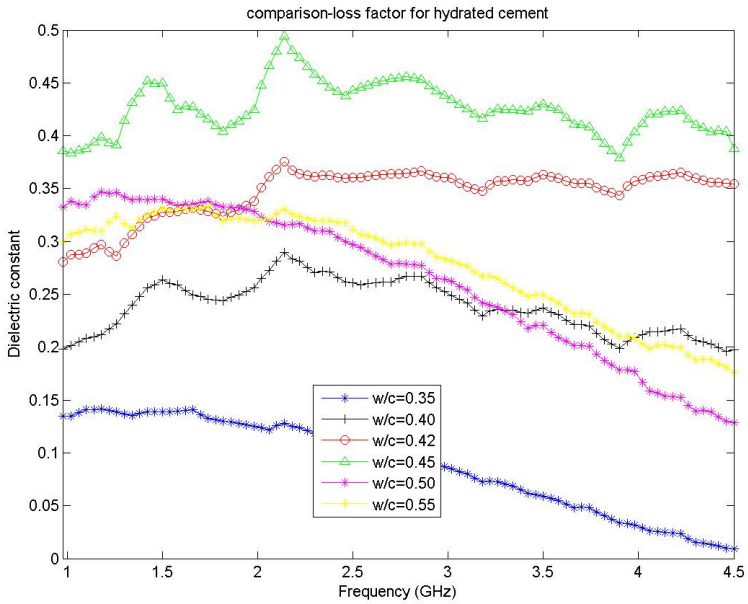

Figure 5-7: Comparison of loss factor of hydrated cement with different w/c ratios

lating dielectric properties of host material in our case? In this section, a numerical method is introduced to verify the effectiveness of M-G's model on dielectric constant of host material.

The numerical method has two steps. First, a mathematical equation is obtained by curve fitting dielectric constant with frequency in the frequency range of 0.98 GHz to 3.5 GHz. Then apply this equation on the dielectric constant in the frequency range of 3.5 GHz to 4.5 GHz and see the error between the results from M-G's model and the mathematical equation.

In curve fitting, the mathematical equation has to fit the results from M-G's model on both values and slope. In addition, the dielectric constant calculated from the mathematical equation has to be greater than zero at all the frequencies. Base on these requirements, exponential function is selected to do curve fitting. The equation is shown

in Eq. 5-2.

$$\epsilon_r'(\omega) = a \times exp(b \times \omega) \tag{5.2}$$

where,

$\epsilon_r'(\omega)$ = Dielectric properties from mathematical equation

ω = Frequency (GHz)

a and b = Coefficients of mathematical equation

Hydrated cement with w/c ratio of 0.35 is used as an example for showing the results from curve fitting. The mathematical equation for hydrated cement with w/c ratio of 0.35 is shown in Eq. 5-3. We can see that the dielectric constant from Eq. 5-3 will always be no less than zero and it is decreased with the increase of the frequency which is consistent with the theory of dielectric dispersion. In addition, the slope of Eq. 5-3 is also decreased with the increase of the frequency which agrees with data from M-G's model. The curve fitting result in the frequency range of 0.98 GHz to 3.5 GHz is shown in Figure 5-8. After curve fitting, dielectric constant in the frequency range of 3.5 GHz to 4.5 GHZ is calculated by plugging frequencies into Eq. 5-3 and the results are shown in Figure 5-9. It is observed that the dielectric constant from Eq. 5-3 and M-G's model has good agreement in both values and slope.

$$\epsilon_r'(\omega) = 7.311 \times exp(-0.01256 \times \omega) \tag{5.3}$$

where,

$\epsilon_r'(\omega)$ = Dielectric properties from mathematical equation for hydrated cement with w/c ratio of 0.35

ω = Frequency (GHz)

7.311 and −0.01256 = Coefficients of mathematical equation

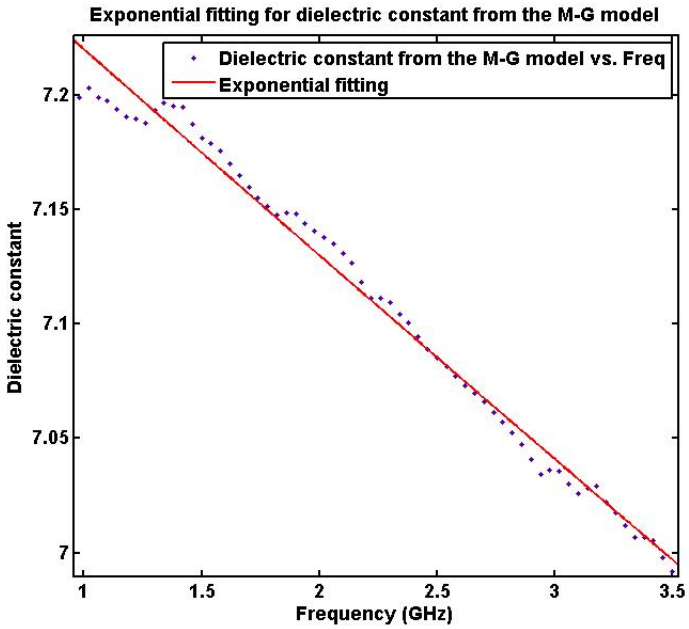

Figure 5-8: Curve fitting of dielectric constant of hydrated cement for w/c ratio of 0.35

For the other w/c ratios, curve fitting results also provide good agreement with results from M-G's model with different coefficients of *a* and *b*. The values of *a* and *b* are shown in Table 5.5.

In conclusion, by using the numerical method, the effectiveness of M-G's model in calculating the dielectric constant of host material in our case is verified. For loss factor part, there is no method to verify the effectiveness of M-G's model.

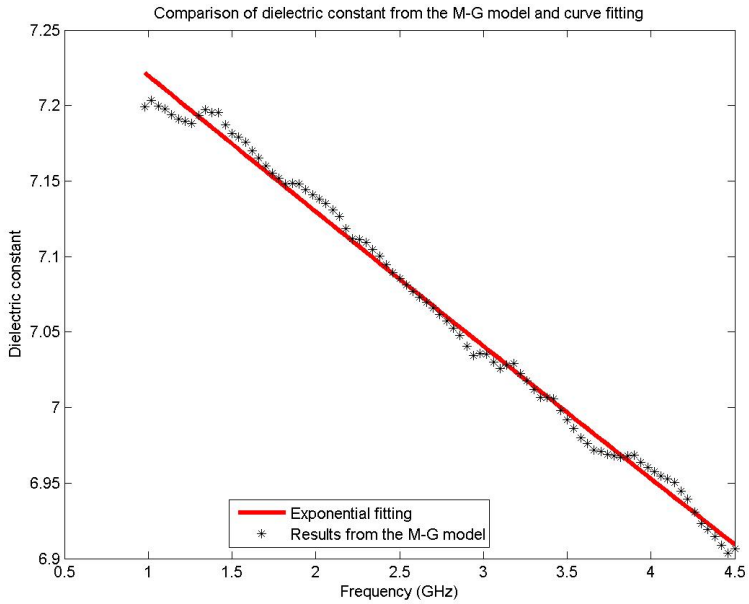

Figure 5-9: Comparison of dielectric constant of hydrated cement from M-G's model and exponential curve fitting - w/c=0.35

5.2 Wiener's Model

Wiener's model is a two-phase dielectric model for mixing material and it is a semi-empirical formula derived from form factors. Different shapes of the inclusion material have different form factors according to depolarization factors of the inclusion. Therefore, Wiener's model can be only used on oven-dried cement paste panels which have only two phases, air and hydrated cement. The equation of Wiener's model is shown in Eq. 5-4.

$$\frac{\epsilon - \epsilon_h}{\epsilon + u} = V_i \times \frac{\epsilon_i - \epsilon_h}{\epsilon_i + u} \tag{5.4}$$

ϵ = Dielectric properties of the mixing material

ϵ_h = Dielectric properties of the host material

ϵ_i = Dielectric properties of the inclusion material

Table 5.2: Coefficients of curve fitting on results from M-G's model

Sample	a	b
CP35	7.311	-0.01256
CP40	10.28	-0.01575
CP42	9.158	-0.01845
CP45	9.915	-0.01906
CP50	10.02	-0.01252
CP55	11.76	-0.01231

V_i = Volumetric ratio of the inclusion material

u = Form factor of the inclusion material

About the form factor u, Eq. 5.5 to Eq. 5.7 show the form factor u for sphere inclusion, disk inclusion and needle inclusion, respectively. We can see that if the shape of the inclusion material is assumed to be sphere and plug Eq. 5-5 into Eq. 5-4 to replace u, the equation of M-G's model can be obtained. The results of M-G's model are discussed above.

$$u = 2 \times \epsilon_h \tag{5.5}$$

$$u = 2 \times \epsilon_i \tag{5.6}$$

$$u = 0.5 \times (\epsilon_i - 3 \times \epsilon_h) \tag{5.7}$$

Similarly as M-G's model, we know the dielectric properties of the mixing material from experimental measurements, as well as the dielectric properties of the inclusion material which is air. Thus in this section, Wiener's model is also used in the inverse way such that we can calculate the dielectric properties of host material which is hy-

drated cement in this case. The shape of the inclusion material is assumed to be either disk or needle, and we can compare the dielectric properties of host material from different shapes of the inclusion.

5.2.1 Results of Wiener's Model on Oven-dried Cement Paste Panels - Disk Inclusion

Assuming the shape of the inclusion material to be disk, we can get the dielectric properties of the host material for each w/c ratio. However, for w/c ratio except 0.35, the dielectric constants of the host material are all negative which is not correct. Figure 5-10 is an example which shows the curve of the dielectric constant with the frequency for the host material with w/c ratio of 0.40 from Wiener's model. We can see that the values of the dielectric constant are all negative. The reason is probably because the volumetric ratio of the inclusion material in oven-dried cement paste panels is greater than 50% except w/c ratio of 0.35. In summary, disk inclusion does not work in modeling the dielectric properties of oven-dried cement paste panels.

5.2.2 Results of Wiener's Model on Oven-dried Cement Paste Panels - Needle Inclusion

Assuming the shape of the inclusion material to be needle, we can also use the inverse way of Wiener's model to calculate the dielectric properties of the host material for each w/c ratio.

Figure 5-11 and Figure 5-12 show the comparisons of the dielectric constant and

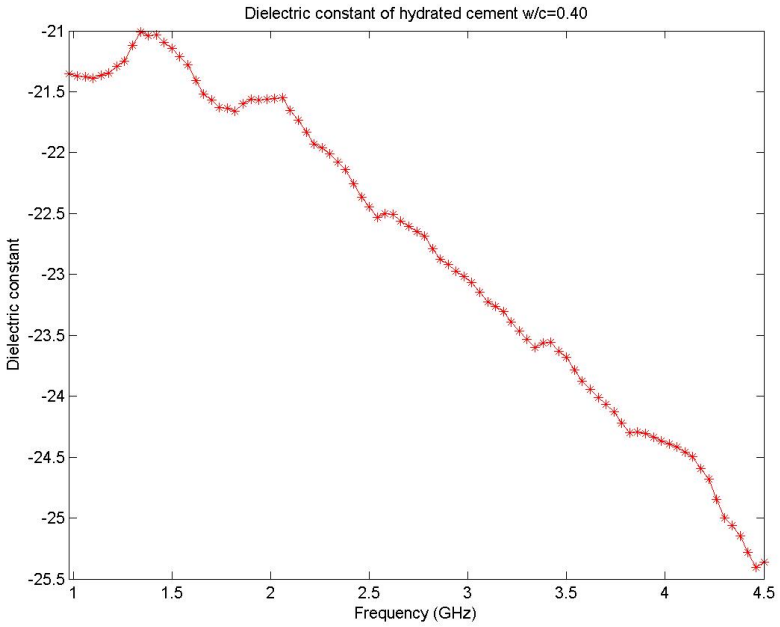

Figure 5-10: Dielectric constant of hydrated cement from Wiener's model - w/c=0.40 - disk inclusion

loss factor for the host material, respectively. We can see that the dielectric constant of the host material increases with the w/c ratio in general. This trend is also as similar as the dielectric constant of the mixing material (oven-dried cement paste panels) and the dielectric constant of the host material from M-G's model. Nevertheless, the loss factor still does not have obvious trend.

Also, we can compare the dielectric properties of the host material from sphere inclusion and needle inclusion for each w/c ratio. The dielectric constants of the host material from needle inclusion are all less than those from sphere inclusion for the same w/c ratio at the same frequency. This is also true for the loss factor of the host material from sphere inclusion and needle inclusion. Figure 5-13 and Figure 5-14 show the comparisons of the dielectric properties of the host material with w/c ratio of 0.35. The

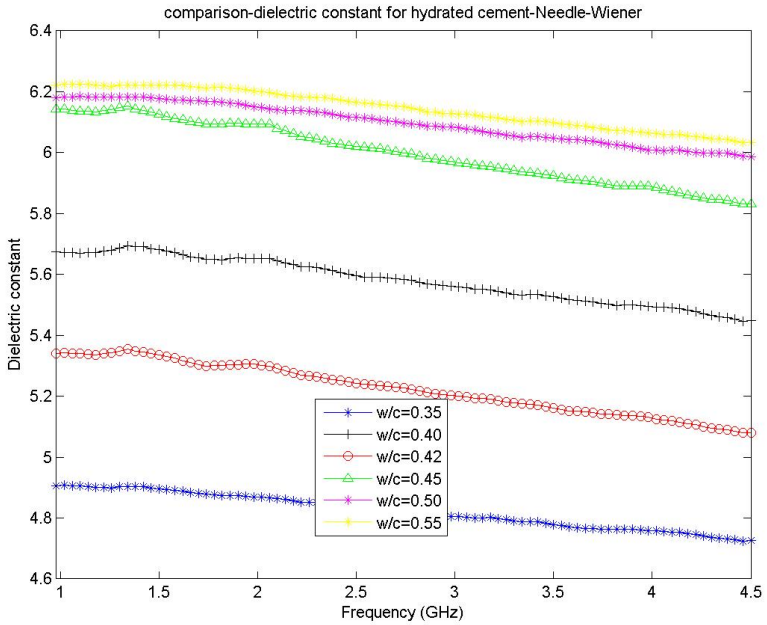

Figure 5-11: Comparison of dielectric constant for hydrated cement from Wiener's model - needle inclusion

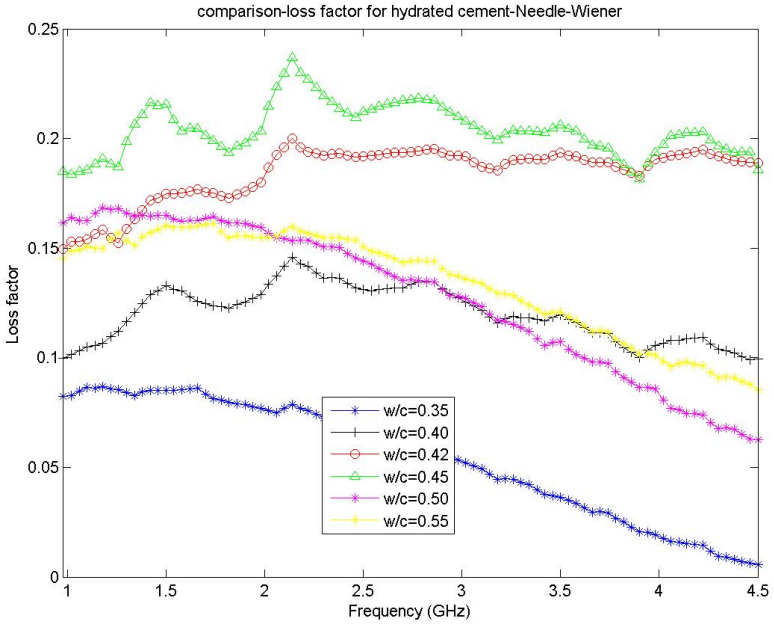

Figure 5-12: Comparison of loss factor for hydrated cement from Wiener's model - needle inclusion

comparison from the other w/c ratios are similar. The only reason for the difference is the shape of the inclusion material. Therefore the shape of the inclusion material does have significant influence on calculation of the dielectric properties of the host material using the inverse way of Wiener's model.

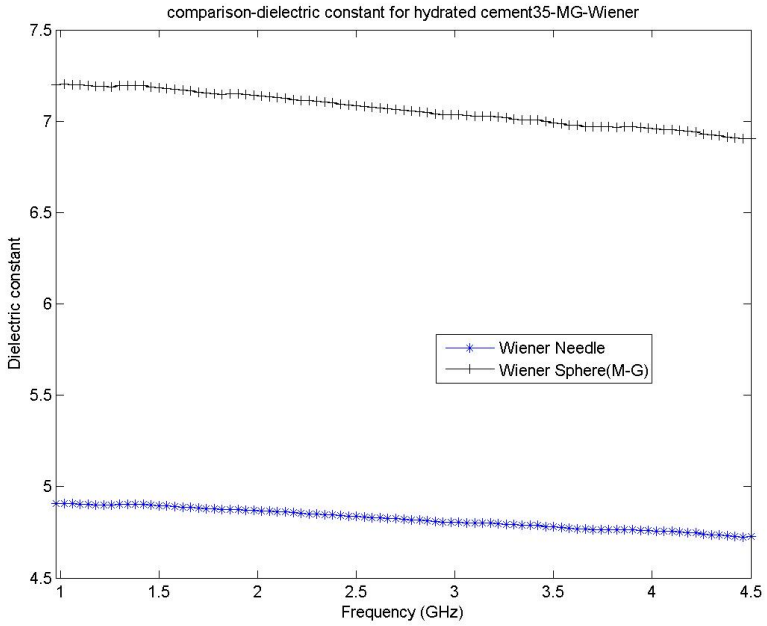

Figure 5-13: Comparison of dielectric constant for hydrated cement from sphere inclusion and needle inclusion

5.3 Polder-van Santen's Model

In this section, Polder-van Santen's model is applied on the dielectric properties of room-conditioned cement paste panels which can be considered as a three-phase material. The objective is to see what depolarization factors can lead to the modeling results which are close to experimental measurements.

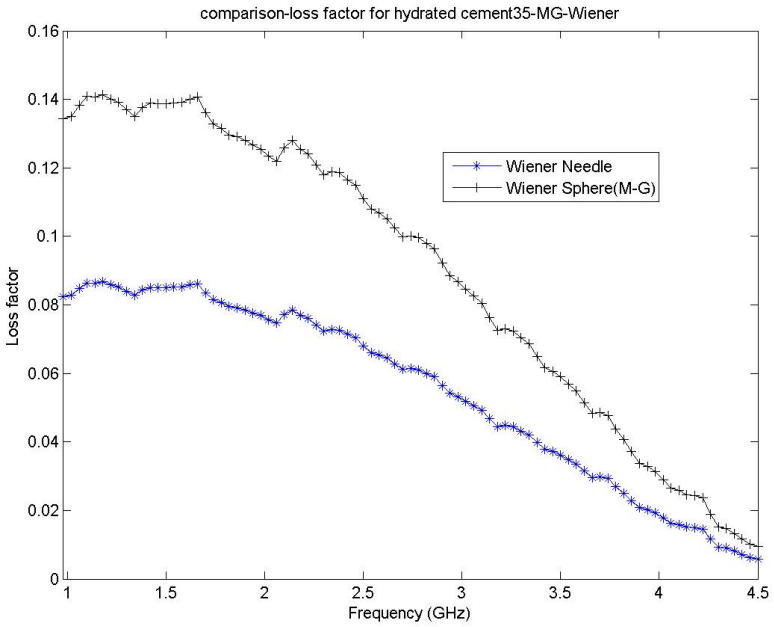

Figure 5-14: Comparison of loss factor for hydrated cement from sphere inclusion and needle inclusion

5.3.1 Approach of Polder-van Santen's Model on Room-conditioned Cement Panels

Polder-van Santen's model is a multiple-phase model for arbitrary shapes of the inclusion materials which are orientated at random in the host material. The mathematical expression of Polder-van Santen's model is shown in Eq. 5.8.

$$\epsilon - \epsilon_h = \sum_{i=1}^{N} V_i \times (\epsilon_i - \epsilon_h) \times 1/3 \times \sum_{j=1}^{3} \frac{\epsilon}{\epsilon + N_j \times (\epsilon_i - \epsilon)} \tag{5.8}$$

ϵ = Dielectric properties of the mixing material

ϵ_h = Dielectric properties of the host material

ϵ_i = Dielectric properties of the *ith* inclusion material

V_i = Volumetric ratio of the *ith* inclusion material

N_j = Depolarization factors for the *ith* inclusion material

Hydrated cement is also the host material in this case. The dielectric properties of the host material were calculated from M-G's model (sphere inclusion) and Wiener's model (needle inclusion), and the dielectric properties of the inclusion materials, air and water, can be obtained from experimental measurements. In addition, we have experimental results of the mixing material, room-conditioned cement paste panels, from the coaxial probe measurements. Also, the volumetric ratio of air and water can be experimentally determined by ASTM C642.

As to the depolarization factors, they are only dependent on the ratios of the semi-axes of the ellipsoids from Sihvola *et. al.* (1988) [24]. The depolarization factors must satisfy $N_1 + N_2 + N3 = 1$ without negative numbers. For the depolarization factors of air, two extreme cases are considered in this thesis, sphere and needle. For sphere, the depolarization factors are (1/3, 1/3, 1/3), and they are (0, 1/2, 1/2)[24, 20] for needle. For the depolarization factors of water, they have to be assumed.

Since it is complex to get the mathematical expression of ϵ from Eq. 5-8 in terms of ϵ_i, ϵ_h, V_i, and N_j, the parameters are plugged into the left-hand side and right-hand side of Eq. 5-8 separately and see how close the results will be by assuming different depolarization factors of water. The flowchart is shown in Figure 5-15.

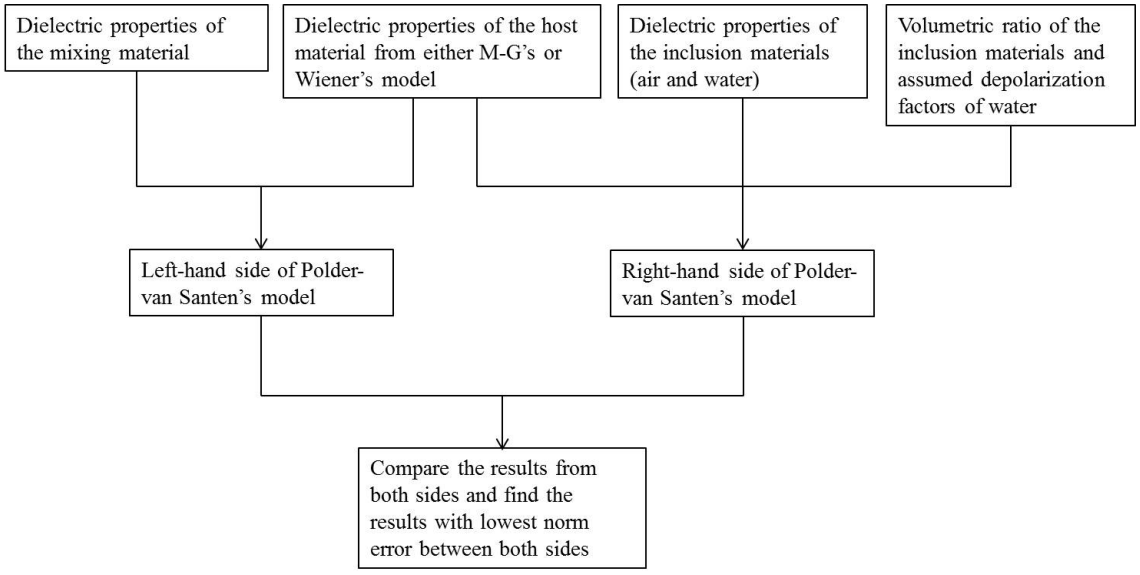

Figure 5-15: Process of Polder-van Santen's model

5.3.2 Results of Polder-van Santen's Model on Room-conditioned Cement Panels

First, air is assumed to be sphere and the dielectric properties of the host material from M-G's model are plugged into Eq. 5-8. The results on the room-conditioned cement paste panel with w/c ratio of 0.35 are used as an example. Figure 5-16 shows the comparison results of real and imaginary parts from left-hand side and right-hand side of Eq. 5-8. We can see that the curves of real part from left-hand side and right-hand side have similar trend, but very different values. The imaginary part from left-hand side and right-hand side also has very different values. The depolarization factors of water which lead to the final results are (0.35,0.35,0.3) which are close to the depolarization factors of sphere inclusion.

Figure 5-17 to Figure 5-21 show the results from room-conditioned cement paste

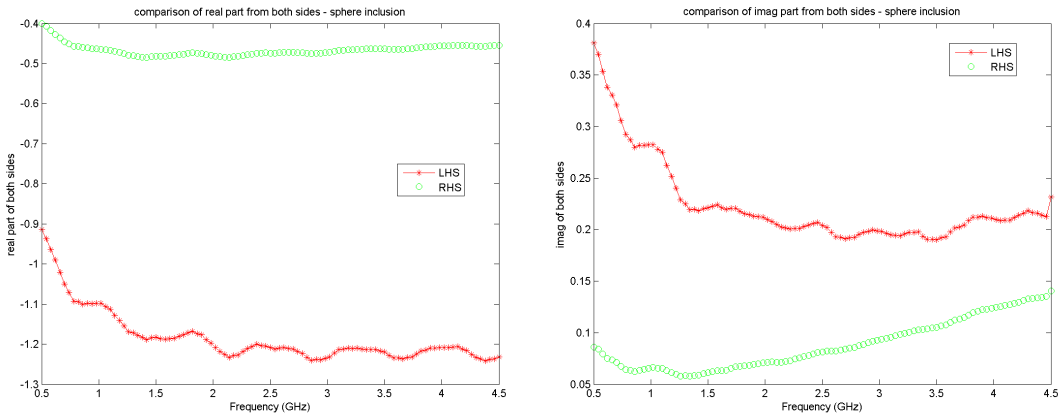

Figure 5-16: Results of room-conditioned CP35 from Polder-van Santen's model - spherical air

panels with the w/c ratios of 0.40, 0.42, 0.45, 0.50, and 0.55, respectively. We can see that none of these can provide close results from right-hand side with the results from left-hand side if the shape of air is assumed to sphere.

Table 5.3 shows the determined depolarization factors of water if the shape of air is assumed to be sphere. We can see that the depolarization factors of water are all very close to those of sphere inclusion.

Table 5.3: Depolarization factors of water from sphere inclusion of air

Sample	Depolarization factors
CP35	(0.35,0.35,0.3)
CP40	(0.3,0.35,0.35)
CP42	(0.3,0.35,0.35)
CP45	(0.35,0.45,0.2)
CP50	(0.3,0.3,0.4)
CP55	(0.35,0.3,0.35)

Second, air is assumed to be needle and the dielectric properties of the host material from Wiener's model are plugged into Eq. 5-8. The results on the room-conditioned

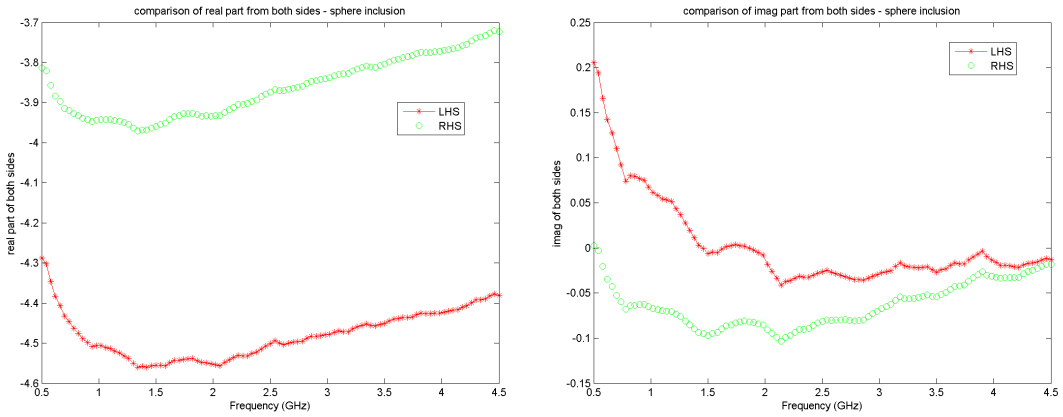

Figure 5-17: Results of room-conditioned CP40 from Polder-van Santen's model - spherical air

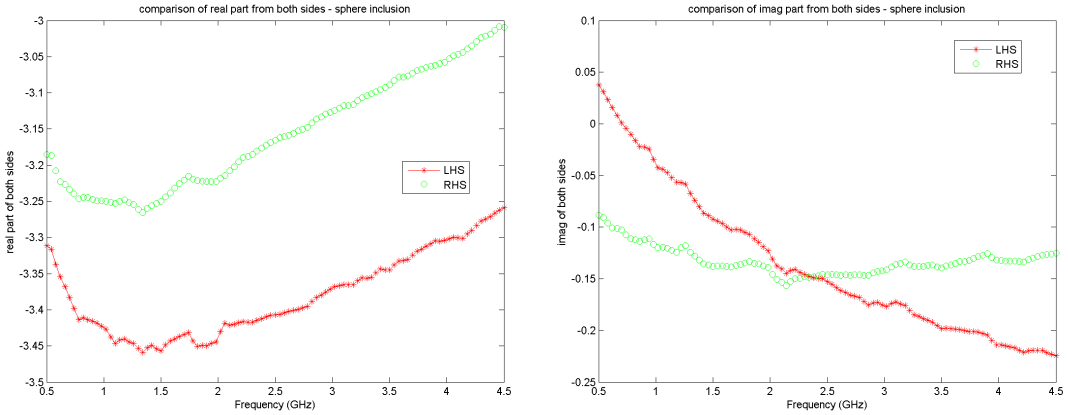

Figure 5-18: Results of room-conditioned CP42 from Polder-van Santen's model - spherical air

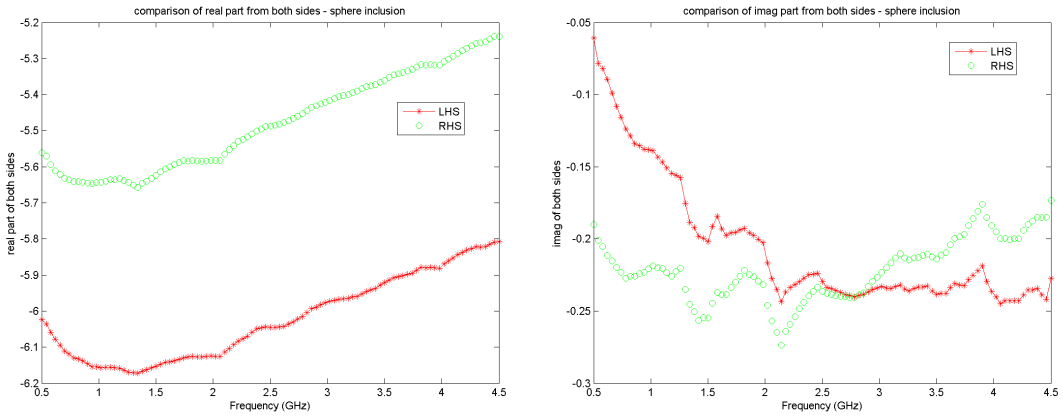

Figure 5-19: Results of room-conditioned CP45 from Polder-van Santen's model - spherical air

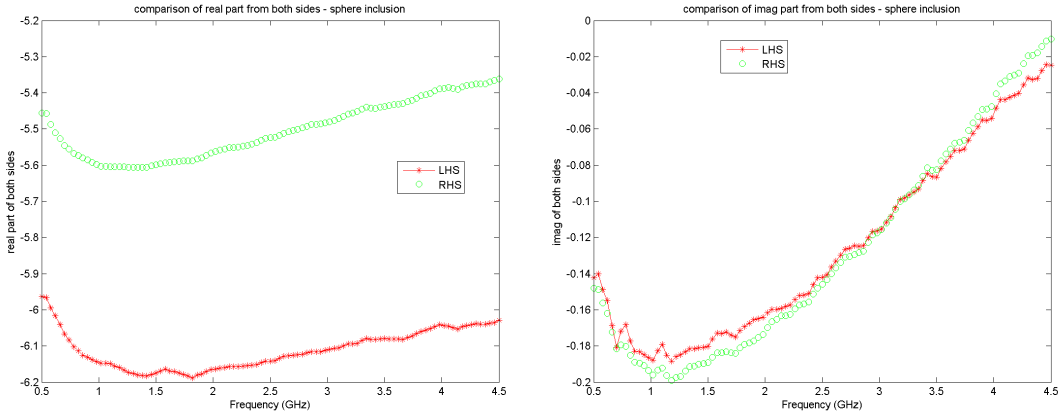

Figure 5-20: Results of room-conditioned CP50 from Polder-van Santen's model - spherical air

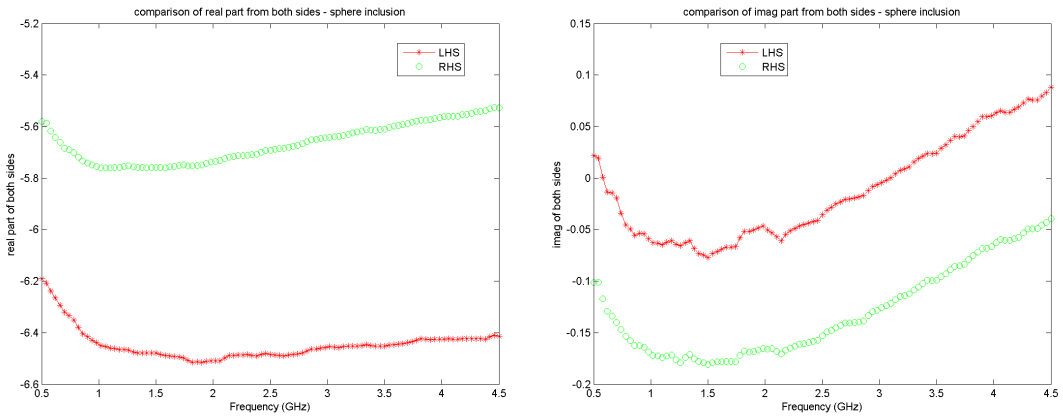

Figure 5-21: Results of room-conditioned CP55 from Polder-van Santen's model - spherical air

cement paste panel with w/c ratio of 0.35 are used as an example. Figure 5-16 shows the comparison results of real and imaginary parts from left-hand side and right-hand side of Eq. 5-8. We can see that the real part from left-hand side and right-hand side is closer even though the trend is not the same. The imaginary part from left-hand side and right-hand side also has different trends. The depolarization factors of water which lead to the final results are (0.75,0.15,0.1).

Figure 5-23 to Figure 5-27 show the results from room-conditioned cement paste panels with the w/c ratios of 0.40, 0.42, 0.45, 0.50, and 0.55, respectively. We can see that if the shape of air is assumed to be needle, the real part has close results between left-hand side and right-hand side, but the imaginary part still has no good results.

Table 5.4 shows the determined depolarization factors of water if the shape of air is assumed to be needle. We can see that the the largest values of the depolarization factors of water are all close to each other.

Comparing the results of Polder-van Santen's model by assuming the shape of air

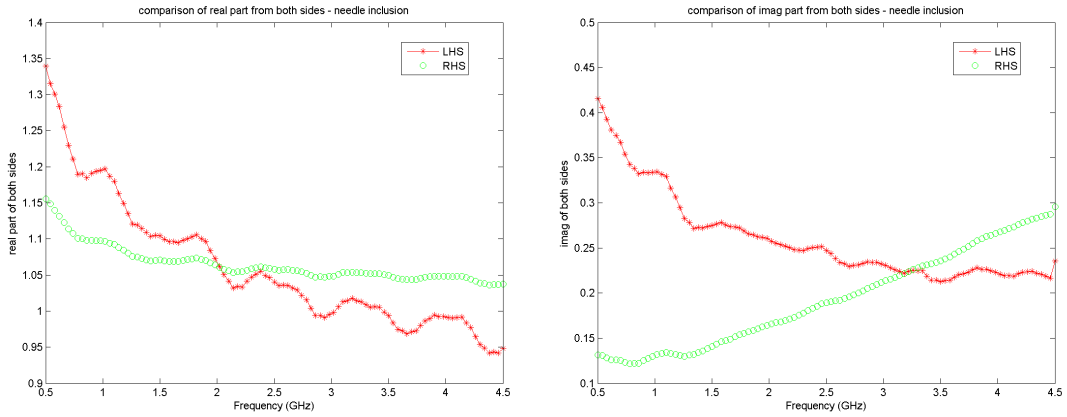

Figure 5-22: Results of room-conditioned CP35 from Polder-van Santen's model - needle air

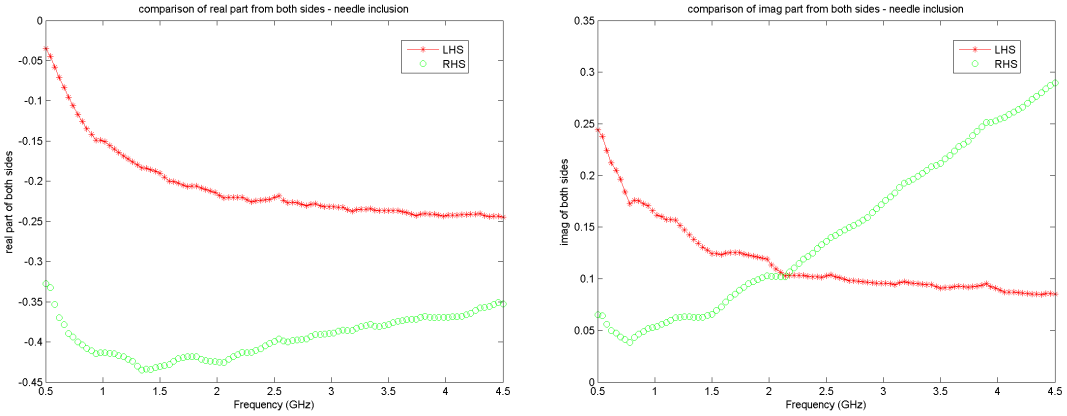

Figure 5-23: Results of room-conditioned CP40 from Polder-van Santen's model - needle air

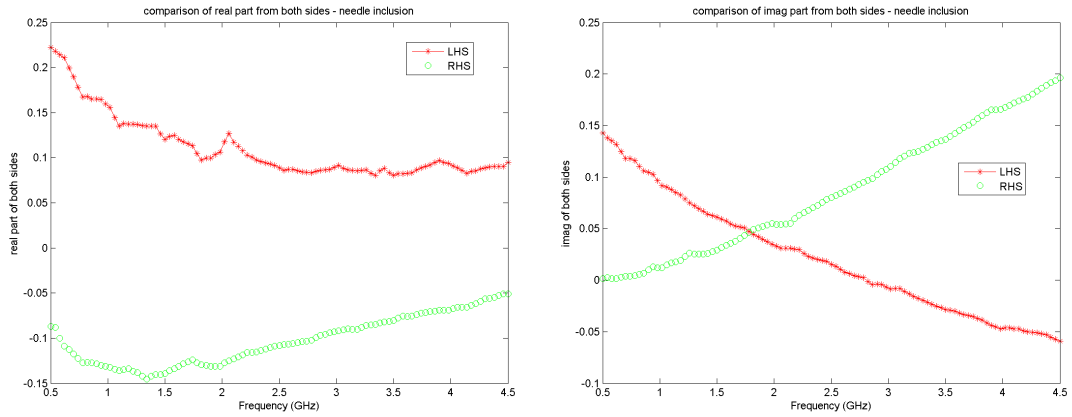

Figure 5-24: Results of room-conditioned CP42 from Polder-van Santen's model - needle air

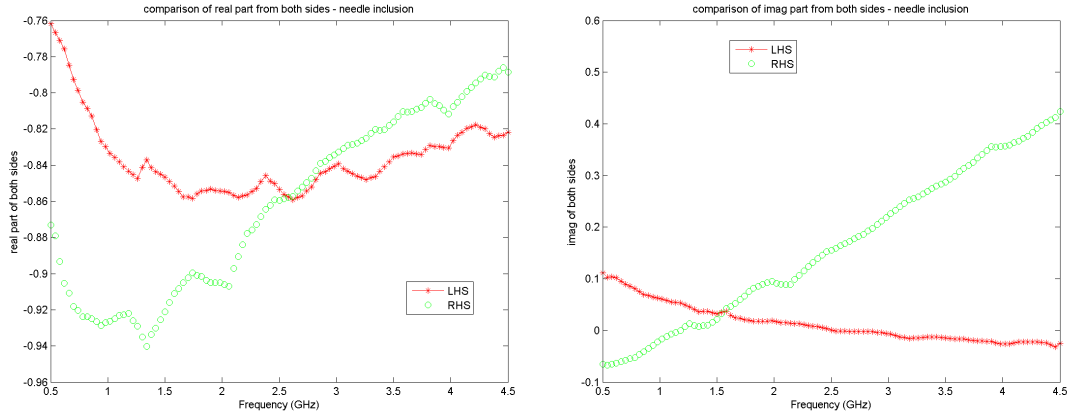

Figure 5-25: Results of room-conditioned CP45 from Polder-van Santen's model - needle air

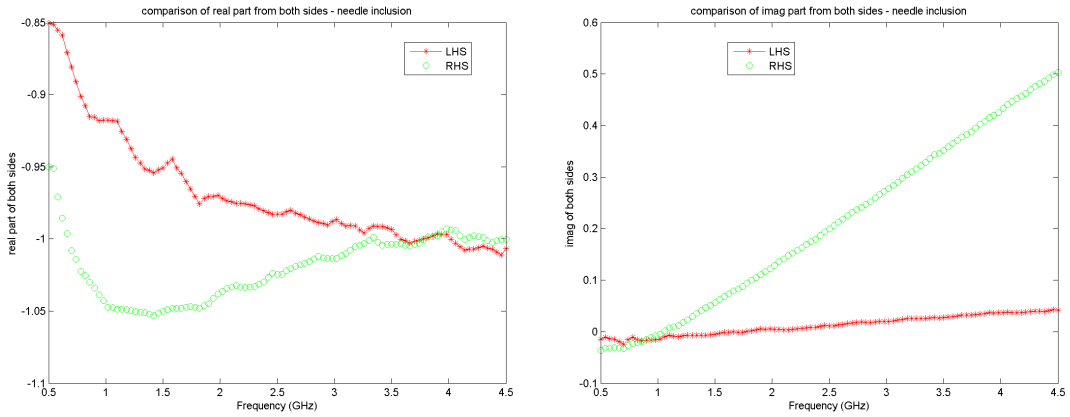

Figure 5-26: Results of room-conditioned CP50 from Polder-van Santen's model - needle air

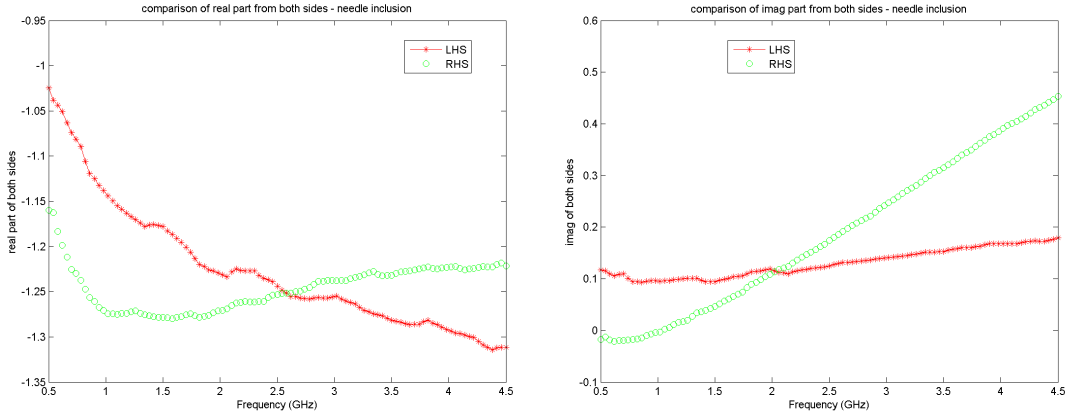

Figure 5-27: Results of room-conditioned CP55 from Polder-van Santen's model - needle air

Table 5.4: Depolarization factors of water from needle inclusion of air

Sample	Depolarization factors
CP35	(0.75,0.15,0.1)
CP40	(0.05,0.85,0.1)
CP42	(0.05,0.85,0.1)
CP45	(0.2,0.8,0)
CP50	(0,0.8,0.2)
CP55	(0.3,0.7,0)

to be sphere or needle, we can see that better results with less norm error are from the assumption that the shape of air is needle. Table shows 5.4 norm errors between left-hand side and right-hand side. We can see that if the shape of air is assumed to be needle, better results are provided.

Table 5.5: Norm error from spherical air and needle air

Sample	Norm error (sphere)	Norm error (needle)
CP35	7.1	1.2
CP40	7.0	3.1
CP42	2.9	3.1
CP45	5.7	2.9
CP50	6.2	3.2
CP55	9.1	2.2

5.4 Summary

From this chapter, by assuming the shape of the air in oven-dried cement paste panels to be sphere or needle, we can calculate the dielectric properties of the host material which is the hydrated cement in the inverse way of M-G's model or Wiener's model. We can see that the dielectric properties of the host material are different from spherical inclusion and needle inclusion due to different form factors. Also, the dielectric

constant of the host material shows the descending trend in general which is similar as the overall dielectric constant.

In addition, Polder-van Santen's model was used for modeling the dielectric properties of room-conditioned cement paste panels. Hydrated cement is also the host material in room-conditioned cement paste panels. There is one more phase which is water. By plugging the dielectric properties of the host material from M-G's model or Wiener's model and air into Polder-van Santen's model, the dielectric properties of room-conditioned cement paste panels from experimental measurements, and depolarization factors for sphere or needle inclusion, we can calculate the results from left-hand side and right-hand side. The depolarization factors of water are assumed. From the results, we can see that the dielectric properties of the host material by using Wiener's model and assuming the shape of air to be needle can provide better modeling results on room-conditioned cement paste panels. The depolarization factors of water which can lead to the modeling results are stable in general.

Chapter 6

Conclusions, Future Work and Contribution

In this chapter, conclusions and contributions from the research work in this thesis are summarized. Also, future work is recommended.

6.1 Conclusions

The conclusions drawn from this thesis are as following.

1. Yu's model can provide the best modeling results of dielectric modeling on both oven-dried and room-conditioned cement paste panels among the homogeneous models in this thesis. Debye's model, Havriliak-Negami's model and Yu's model can provide us with similar results on dielectric constant, but Yu's model has the best performance on loss factor part.

2. The model parameters, ϵ_∞ and ϵ_s are similar from Debye's model and Havriliak-

Negami's model. However, τ from these two models are different.

3. The dielectric properties of the host material calculated from Maxwell-Garnett's model and Wiener's model are different if the shapes of the inclusion material are assumed to be different for oven-dried cement paste panels.

4. From the results of Polder-van Santen's model, the dielectric properties of the host material by assuming the shape of air to be needle can lead to better performance on dielectric modeling of room-conditioned cement paste panels.

6.2 Future Work

Based on the conclusions drawn in the thesis, several future works are recommended.

1. The algorithm to determine τ needs to be improved since different homogeneous models gave us very different values of τ, and it is an important model parameter.

2. It is better to involve moisture content in dielectric modeling as one more parameter since moisture content has significant influence on dielectric properties of cementitious materials.

3. Better understanding and more applications are needed to use heteroecious dielectric models.

4. More experimental data is necessary to improve the accuracy of dielectric models.

6.3 Contributions

1. Introduced a new method to apply Debye's model on hydrated cement paste panels and calculate modeling parameters. The method can provide good agreement with experimental data on dielectric constant.

2. Involved w/c ratio in Yu's model and found that Yu's model had better performance for hydrated cement paste panels than the other two models in this thesis without involving w/c ratio.

3. Used two two-phase heterogeneous models to calculate the dielectric properties of the host material which is hydrated cement in this thesis by assuming different shapes of air. Also, the dielectric properties of the host material were used to verify the dielectric properties of room-conditioned cement paste panels with three phases. The results show that this process has good potential for dielectric modeling on hydrated cement paste panels.

Bibliography

[1] Agilent. Application note: Agilent basics of measuring the dielectric properties of materials. *Agilent Literature Number 5989-2589EN*, June 2006.

[2] Agilent. 85070e dielectric probe kit 200mhz to 50ghz. *Agilent Literature Number 5989-0222EN*, March 2008.

[3] I. L. Al-Qadi, O. A. Hazim, W. Su, and S. M. Riad. Dielectric properties of portland cement concrete at low radio frequencies. *Journal of Materials in Civil Engineering*, 7(3):192–198, August 1995.

[4] I. L. Al-Qadi, S. Lahouar, and A. Loulizi. In situ measurements of hot-mix asphalt dielectric properties. *NDT&E International*, 34:427–434, 2001.

[5] ASTM. ASTM C642 : Standard test method for density, absorption and voids in hardened concrete. *ASTM International, West Conshohocken, PA, DOI:10.1520/C0642-13, www.astm.org*, 2006.

[6] J. H. Bungey. Sub-surface radar testing of concrete: a review. *Construction and Building Materials*, 18:1–8, 2004.

[7] C. W. Chang, C. H. Lin, and H. S. Lien. Measurement radius of reinforcing steel bar in concrete using digital image gpr. *Construction and Building Materials*, 23:1057–1063, 2009.

[8] W. Chen, P. Shen, and Z. Shui. Determination of water content in fresh concrete mix based on relative dielectric constant measurement. *Construction and Building Materials*, 34:306–312, 2012.

[9] Y. E. Hafiane, A. Smith, P. Abelard, J. P. Bonnet, and P. Blanchart. Dielectric characterization at high frequency (1 mhz - 1.8 ghz) of a portaland cement at the early stages of hydration. *Ceramics - Silikáty*, 43(2):48–51, 1999.

[10] N. E. Hager and R. C. Domszy. Monitoring of cement hydration by broadband time-domain-reflectometry dielectric spectroscopy. *Journal of Applied Physics*, 96(9):5117–5128, November 2004.

[11] V. Janoo, C. Korhonen, and M. Hovan. Measurement of water content in portland cement concrete. *Journal of Transportation Engineering*, 125(3):245–249, May/June 1999.

[12] G. Klysz, J. P. Balayssac, and X. Ferrières. Evaluation of dielectric properties of concrete by a numerical fdtd model of a gpr coupled antenna - parametric study. *NDT&E International*, 41:621–631, 2008.

[13] W. L. Lai, S. C. Kou, W. F. Tsang, and C. S. Poon. Characterization of concrete properties from dielectric properties using ground penetrating radar. *Cement and Concrete Research*, 39:687–695, 2009.

[14] S. Laurens, J. P. Balayssac, J. Rhazi, and G. Arliguie. Influence of concrete relative humidity on the amplitude of ground-penetrating radar (gpr) signal. *Materials and Structures*, 35:198–203, May 2001.

[15] G. P. D. Loor. The effect of moisture on the dielectric constant of hardened portland cement paste. *Appl. Sci. Res.*, 9:297–308, 1961.

[16] N. Makul, P. Keangin, P. Rattanadecho, B. Chatveera, and D. K. Agrawal. Micorwave-assisted heating of cementitious materials: Relative dielectric properties, mechanical property, and experimental and numerical hear transfer characteristocs. *International Communications in Heat and Mass Transfer*, 37:1096–1105, 2010.

[17] P. Q. Mantas. Dielectric response of materials: Extension to the debye model. *Journal of the European Ceramic Society*, 19(12):2079–2086, October 1999.

[18] N. Miura, N. Shinyashiki, S. Yagihara, and M. Shiotsubo. Microwave dielectric study of water structure in the hydration process of cement paste. *J. Am. Ceram. Soc*, 81(1):213–216, 1998.

[19] A. Ogunsola, U. Reggiani, and L. Sandrolini. Modelling shilding properties of concrete. In *17th International Zurich Symposium on Electromagnetic Compatibility*.

[20] D. Ploder and J. H. van Santen. The effective permeability of mixtures of solids. *Physica*, XII(5):257–271, 1946.

[21] A. Robert. Dielectric permittivity of concrete between 50 mhz and 1 ghz and gpr measurements for building material evaluation. *Journal of Applied Geophysics*, 40:89–94, 1998.

[22] F. Sagnard and G. E. Zein. In situ characterization of building materials for propagation modeling: Frequency and time response. *IEEE Transactions on Antennas and Propagation*, 53(10):3166–3172, 2005.

[23] L. Sandrolini, U. Reggiani, and A. Ogunsola. Modelling the electrical properties of concrete for shilding effectiveness prediction. *Journal of Physicas D: Applied Physics*, 40:5336–5372, 2007.

[24] A. H. Sihvola and J. A. Kong. Effective permittivity of dielectric mixtures. *IEEE Transactions on Geoscience and Remote Sensing*, 26(4):420–429, July 1988.

[25] I. C. Solak. Determination of dielectric constants of hydrated cement paste and cement mortar using a contact coaxial probe. Master's thesis, University of Massachusetts Lowell, Lowell, MA, 2011.

[26] M. N. Soutsos, J. H. Bungey, S. G. Millard, M. R. Shaw, and A. Patterson. Dielectric properties of concrete and their influence on radar testing. *NDT&E International*, 34:419–425, 2001.

[27] F. Tsui and S. L. Matthews. Analytical modeling of the dielectric properties of concrete for subsurface radar application. *Construction and Building Materials*, 11:149–161, 1997.

[28] S. Wen and D. D. L. Chung. Effect of admixtures on the dielectric constant of cement paste. *Cement and Concrete Research*, 31:673–677, 2001.

[29] S. Wen and D. D. L. Chung. Cement-based materials for stress sensing by dielectric measurement. *Cement and Concrete Research*, 32:1429–1433, 2002.

[30] T. Yu. *Damage Detection of GFRP-Concrete Systems Using Electromagnetic Waves*. Lambert Acadamic Publishing, 2009.